

## Electronic Supplementary Information

### Group 4 permethylindenyl complexes for slurry-phase polymerisation of ethylene

Jessica V. Lamb, Jean-Charles Buffet, Zoë R. Turner and Dermot O'Hare\*

*Chemistry Research Laboratory, Department of Chemistry, University of Oxford, Mansfield Road, Oxford OX1 3TA, United Kingdom. Tel: +44(0) 1865 272686; E-mail: dermot.ohare@chem.ox.ac.uk*

### Table of Contents

1.	General experimental details	S2
1.1	Air- and moisture-sensitive compounds	S2
1.2	Commercially supplied reagents	S2
1.3	Synthesis of literature compounds	S2
1.4	Solvent preparation	S2
1.5	Solution phase NMR spectroscopy	S3
1.6	Solid state NMR spectroscopy	S3
1.7	Single crystal X-ray diffraction	S3
1.8	Elemental analysis	S3
1.9	Infrared spectroscopy	S4
1.10	Mass spectrometry	S4
1.11	Gel-permeation chromatography	S4
1.12	Scanning electron microscopy	S4
1.13	Differential scanning calorimetry	S4
2.	Representative NMR spectra	S5
3.	Additional crystallographic data	S18
3.1	Crystallographic details	S18
3.2	Geometric parameters and numbering scheme used to define the steric effects of the <i>ansa</i> ligand	S18
3.3	Experimental crystallographic data	S19
4.	Additional polymerisation data	S24
4.1	Polymerisation activities and molecular weights tables	S24
4.2	Additional polymerisation graphs	S38
4.3	SEM images	S44
5.	References	S52

## **General Experimental Details**

### *1.1 Air- and moisture-sensitive compounds*

Air- and moisture-sensitive compounds were handled under an inert N<sub>2</sub> atmosphere, using standard Schlenk line techniques and an MBraun Unilab glove box where required.

### *1.1 Commercially supplied reagents*

Bis(*n*-butylcyclopentadienyl)zirconium (Sigma Aldrich), lithiumcyclopentadienyl (Alfer Aesar), lithium cyclopentadienylmethyl (MCAT GmbH), lithium *n*-butylcyclopentadienyl (Sigma Aldrich), *n*-butyllithium (2.5 M in hexanes, Sigma Aldrich), methyl lithium (1.6 M in diethyl ether, Sigma Aldrich), triisobutylaluminium (Sigma Aldrich) and Ind#H (Shanghai Sunway Pharmaceutical Technology Ltd.) were used as supplied. Prior to use, dimethyldichlorosilane (Sigma Aldrich) was degassed and stored over pre-activated 4 Å molecular sieves; zirconium tetrachloride (Sigma Aldrich) and zirconium tetrabromide (Sigma Aldrich) were dried under vacuum at 140 °C for 48 hours under 10<sup>-2</sup> mbar; silica (SCG Chemicals Co., Ltd.) was dried under vacuum; MgAlCO<sub>3</sub>-LDH (SCG Chemicals Co., Ltd.) was calcined at 150 °C under vacuum for 6 hours. Solid MAO (Tosoh Finechem Corporation) was supplied as a slurry in toluene which was dried under vacuum at 10<sup>-2</sup> mbar until dryness prior to use.

### *1.2 Solvent Preparation*

Pentane and benzene were dried using an MBraun SPS-800 solvent purification system, stored over a potassium mirror, and degassed under partial vacuum before use. THF and Et<sub>2</sub>O were distilled from purple Na/Benzophenone, stored over 4 Å molecular sieves, and degassed under partial vacuum before use.

### *1.3 Synthesis of literature compounds*

Potassium benzyl (K(CH<sub>2</sub>C<sub>6</sub>H<sub>5</sub>) was prepared according to a literature procedure and stored at -20 °C.

Deuterated solvents were dried over NaK (benzene-*d*<sub>6</sub>) or CaH<sub>2</sub> (pyridine-*d*<sub>5</sub>), distilled under static vacuum, freeze-thaw degassed and stored over pre-activated 4 Å molecular sieves under N<sub>2</sub>.

### *1.2 Solution phase NMR spectroscopy*

NMR spectroscopy samples of air- and moisture-sensitive compounds were prepared in a glove box and sealed in 5 mm Young's tap NMR tubes.  $^1\text{H}$  NMR spectra were recorded on a Bruker Avance III HD nanobay 400 MHz NMR spectrometer and  $^{13}\text{C}\{^1\text{H}\}$  spectra were recorded on a Bruker Avance III NMR spectrometer. All spectra were recorded at 23 °C and referenced internally to the residual *proto* solvent peak. All spectra are reported relative to tetramethylsilane ( $\delta = 0$  ppm). Two dimensional  $^1\text{H}$ - $^1\text{H}$  and  $^{13}\text{C}$ - $^1\text{H}$  correlation experiments were used, when necessary, to confirm  $^1\text{H}$  and  $^{13}\text{C}$  assignments.

### *1.3 Solid-state NMR spectroscopy*

All samples were prepared in a glove box under a nitrogen atmosphere and sealed in 4 mm  $\text{ZrO}_2$  rotors. Solid-state NMR spectra were recorded by Dr. Nicholas Rees on a Bruker AVIII HD NanoBay 400 MHz Solid-state NMR spectrometer. Samples were spun at the magic angle (54.71°) at spin rates of 10 kHz for  $^{13}\text{C}$  and  $^{29}\text{Si}$  and 15 kHz for  $^{27}\text{Al}$ .  $^{13}\text{C}$  NMR spectra were referenced to adamantane,  $^{27}\text{Al}$  to  $\text{Al}(\text{NO}_3)_3$  and  $^{29}\text{Si}$  to kaolinite.

### *1.4 Single crystal X-ray diffraction*

Single crystal X-ray diffraction data collection and structure determinations were performed by Dr Zoë Turner (University of Oxford). Crystals were mounted on MiTeGen MicroMounts using perfluoropolyether oil and rapidly transferred to a goniometer head on a diffractometer fitted with an Oxford Cryosystems Cryostream open-flow nitrogen cooling device.<sup>1</sup> Data collections were carried out at 150 K using an Oxford Diffraction Supernova diffractometer using mirror-monochromated Cu  $\text{K}\alpha$  radiation ( $\lambda = 1.54178 \text{ \AA}$ ) and the data was processed using CrysAlisPro.<sup>2</sup> The structures were solved using direct methods (SIR-92)<sup>3</sup> or a charge flipping algorithm (SUPERFLIP)<sup>4</sup> and refined by full-matrix least-squares procedures using the Win-GX software suite.<sup>5, 6</sup> Molecular structures were depicted utilising Ortep,<sup>6</sup> with ellipsoids shown at 50% probability. Molecular bond lengths and angles were calculated using Platon.<sup>7, 8</sup>

### *1.5 Elemental Analysis*

Samples were prepared in a glove box and sealed in glass vials under nitrogen. CHN analyses were carried out in duplicate by Mr. Stephen Boyer, London Metropolitan University.

### *1.6 Infrared spectroscopy*

Air-sensitive samples were prepared in the glove box and ground with anhydrous KBr and then formed into discs using a specially designed press and airtight holder. IR spectra were recorded on a Nicolet iS5 ThermoScientific spectrometer (range = 4000-400 cm<sup>-1</sup>, resolution = 1 cm<sup>-1</sup>) in transmission mode. A background spectrum was run prior to the sample in each case and was subtracted from the spectrum.

### *1.7 Mass Spectrometry*

Samples were run as electron impact (EI) and electrospray ionisation (ESI) mass spectra and the data were collected by Prof. James McCullagh or Dr Victor Mikhailov Chemistry Research Laboratory, University of Oxford.

### *1.8 Gel-Permeation Chromatography (GPC)*

Gel permeation chromatography (GPC) samples were collected by Ms Liv Thorbu at Norner AS (Norway) on a high temperature gel permeation chromatograph with a IR5 infrared detector (GPC-IR5). Samples were prepared by dissolution in 1,2,4-trichlorobenzene (TCB) containing 300 ppm of 3,5-di-*tert*-butyl-4-hydroxytoluene (BHT) at 160 °C for 90 minutes and then filtered with a 10 µm SS filter before being passed through the GPC column. The samples were run under a flow rate of 0.5 mL/min using TCB containing 300 ppm of BHT as mobile phase with 1 mg/mL BHT added as a flow rate marker. The GPC column and detector temperature were set at 145 and 160 °C respectively.

### *1.9 Scanning electron microscopy (SEM)*

Scanning electron microscopy (SEM) analysis was performed on a JOEL JSM 6610LV scanning electron microscope with an accelerating voltage of 3.0 kV. Samples were spread on carbon tape adhered to an SEM stage. Before imaging, the samples were coated with a thin platinum layer (20 nm thickness) to prevent charging and to improve image quality.

### *1.10 Differential scanning calorimetry (DSC)*

Differential scanning calorimetry experiments were performed on a Mettler Toledo TGA/DSC 1 System in a temperature range of 25–250 °C at a rate of 5 °C min<sup>-1</sup>.

## 2. Representative NMR Spectra

*E*-Me<sub>2</sub>SB(Cp<sup>n</sup>Bu,I\*)ZrCl<sub>2</sub> (**E-1**)

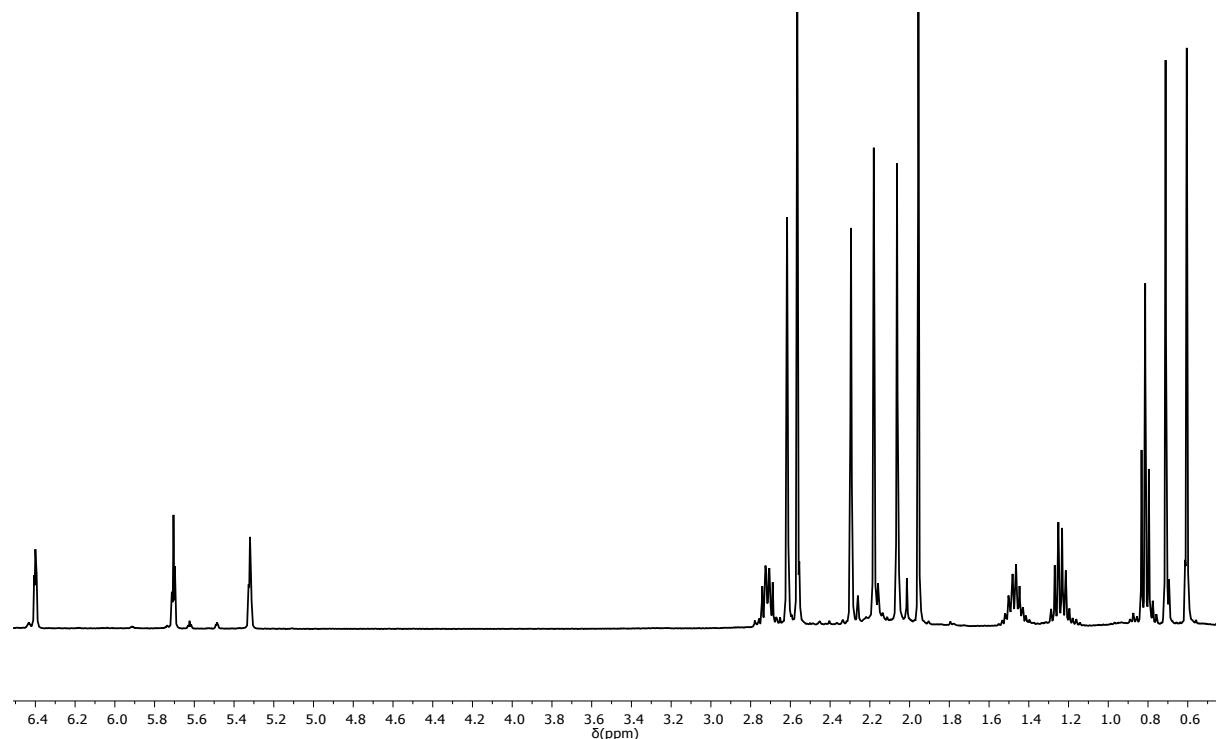


**Fig. S1.** <sup>1</sup>H NMR spectrum (benzene-*d*<sub>6</sub>, 400 MHz, 23 °C) of *E*-Me<sub>2</sub>SB(Cp<sup>n</sup>Bu,I\*)ZrCl<sub>2</sub> (**E-1**).

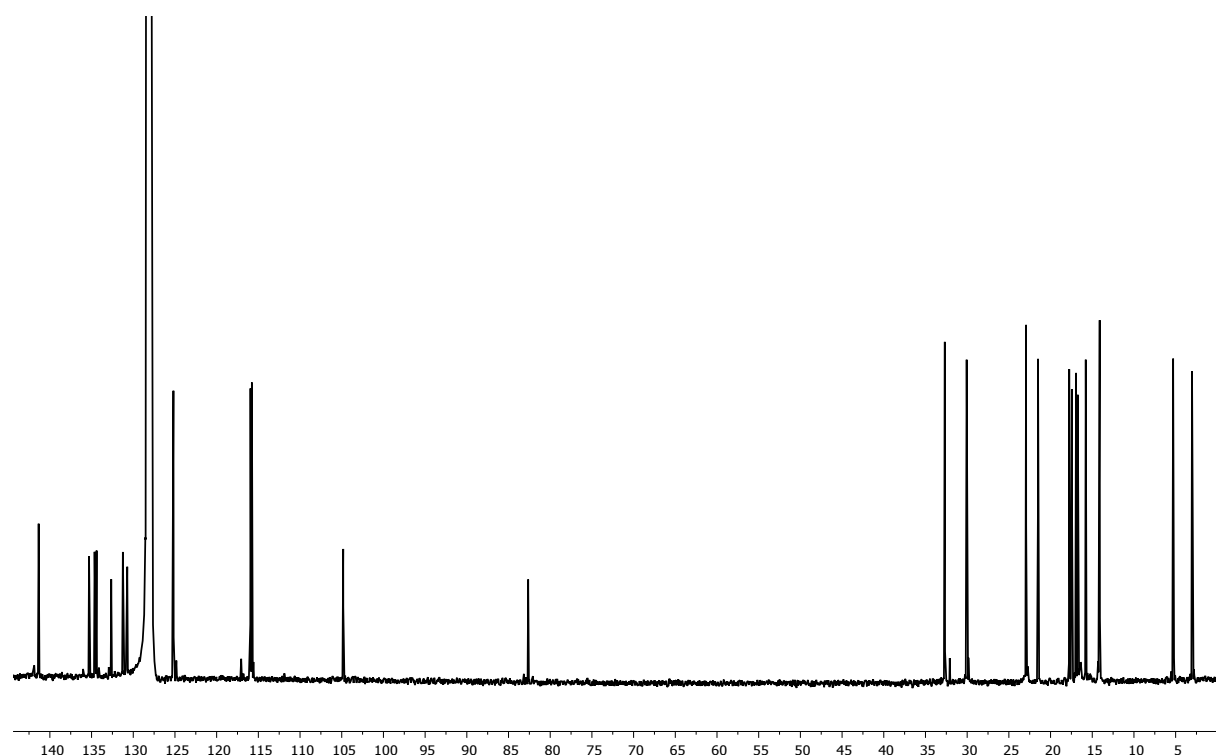


**Fig. S2.** <sup>13</sup>C{<sup>1</sup>H} NMR spectrum (benzene-*d*<sub>6</sub>, 125 MHz, 23 °C) of *E*-Me<sub>2</sub>SB(Cp<sup>n</sup>Bu,I\*)ZrCl<sub>2</sub> (**E-1**).

**Z-Me<sub>2</sub>SB(Cp<sup>nBu</sup>,I\*)ZrCl<sub>2</sub> (Z-1)**

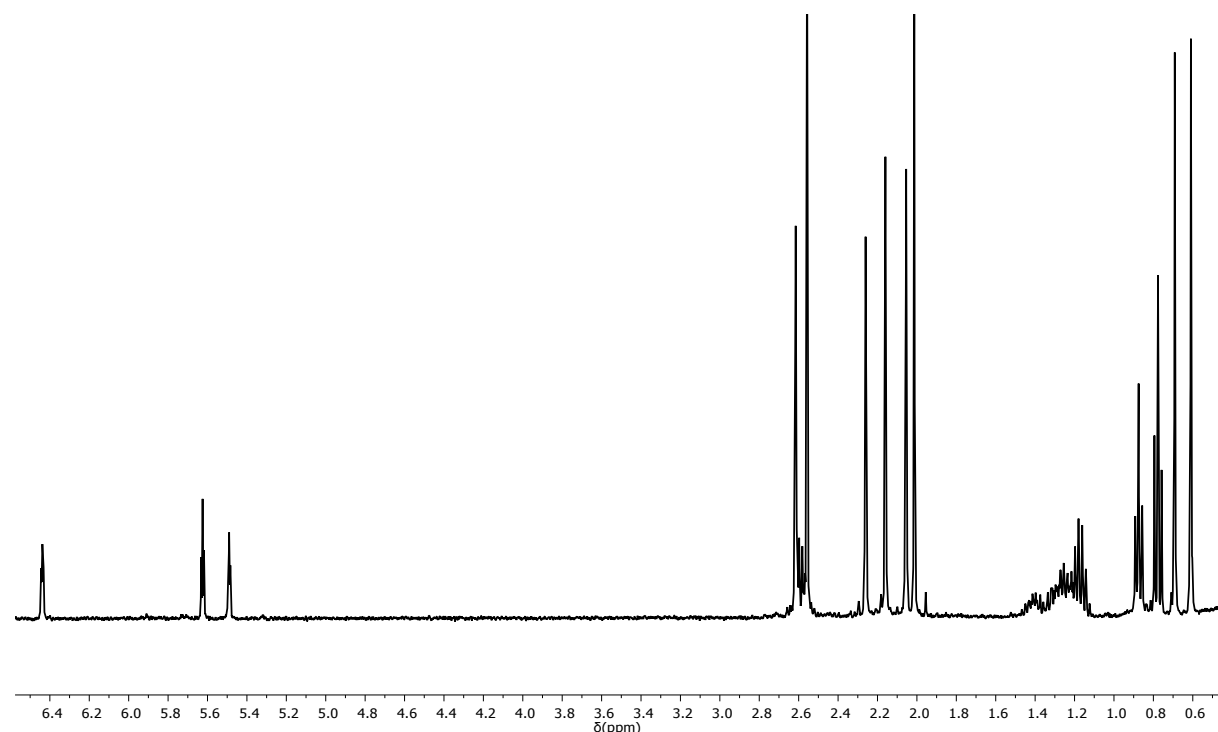


**Fig. S3.** <sup>1</sup>H NMR spectrum (benzene-*d*<sub>6</sub>, 400 MHz, 23 °C) of Z-Me<sub>2</sub>SB(Cp<sup>nBu</sup>,I\*)ZrCl<sub>2</sub> (**Z-1**).

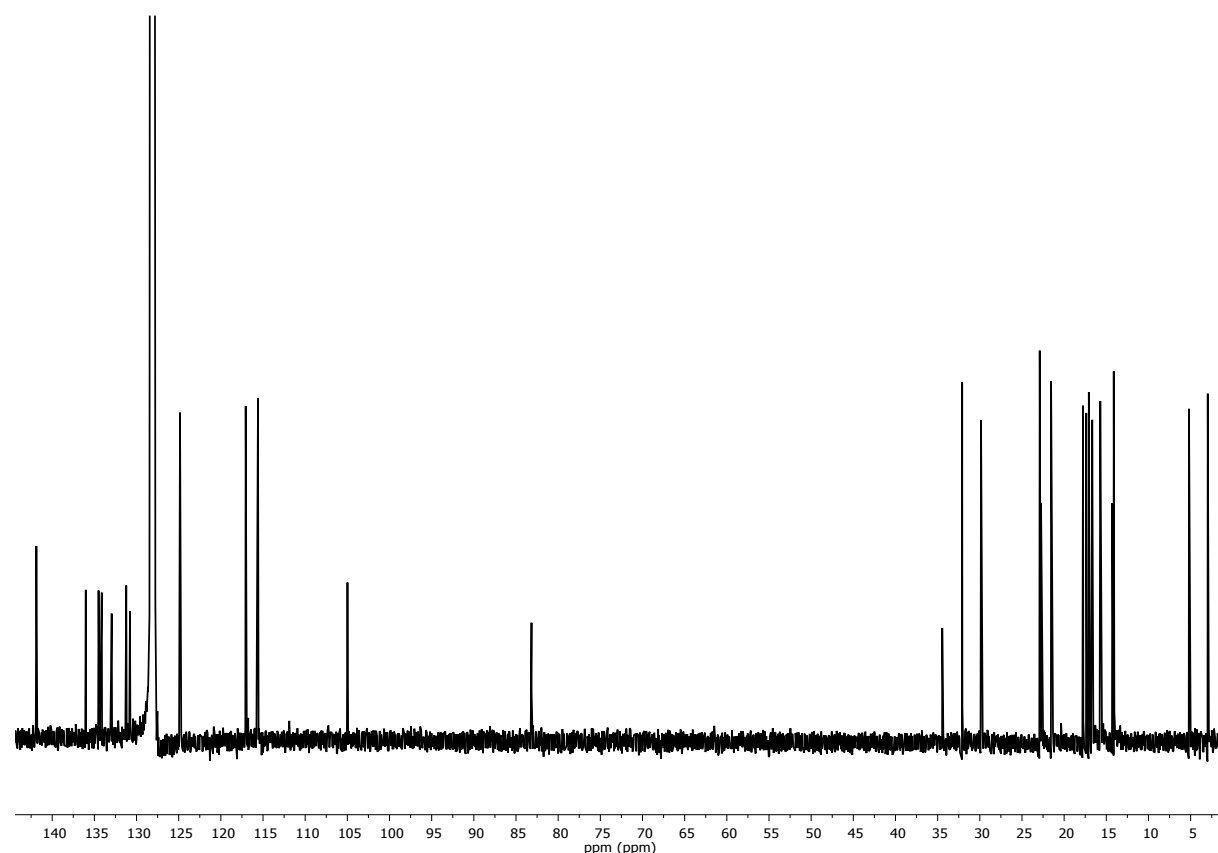


**Fig. S4.** <sup>13</sup>C{<sup>1</sup>H} NMR spectrum (benzene-*d*<sub>6</sub>, 125 MHz, 23 °C) of Z-Me<sub>2</sub>SB(Cp<sup>nBu</sup>,I\*)ZrCl<sub>2</sub> (**Z-1**).

$\text{Me}_2\text{SB}(\text{Cp},\text{I}^*)\text{ZrBr}_2$  (**2**)

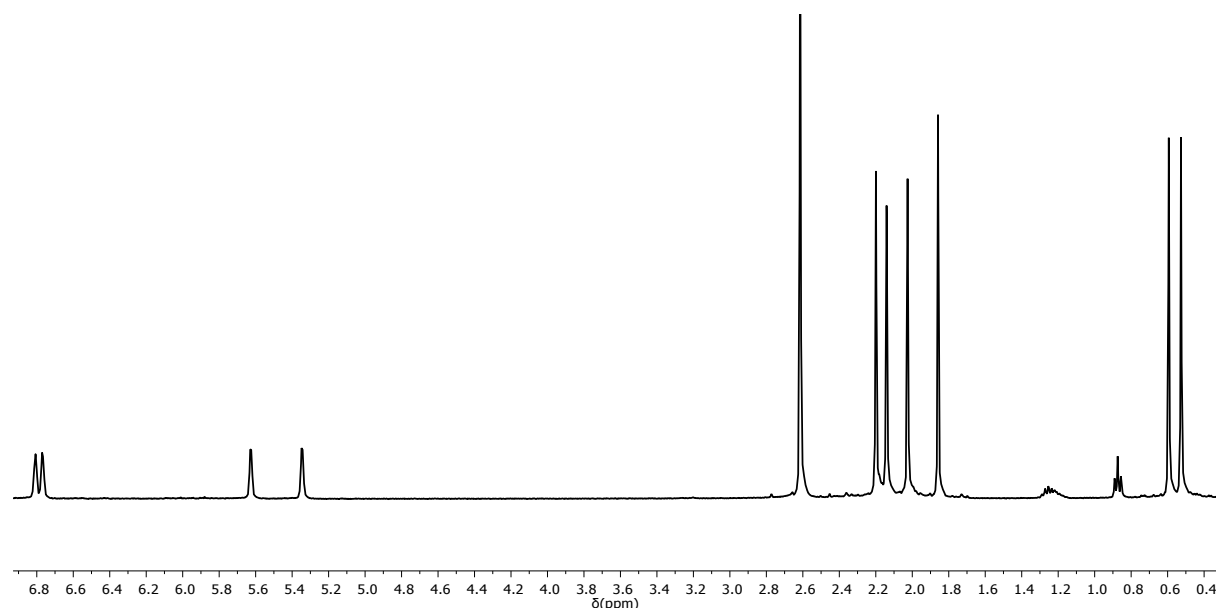


**Fig. S5.**  ${}^1\text{H}$  NMR spectrum (benzene- $d_6$ , 400 MHz, 23 °C) of  $\text{Me}_2\text{SB}(\text{Cp},\text{I}^*)\text{ZrBr}_2$  (**2**).

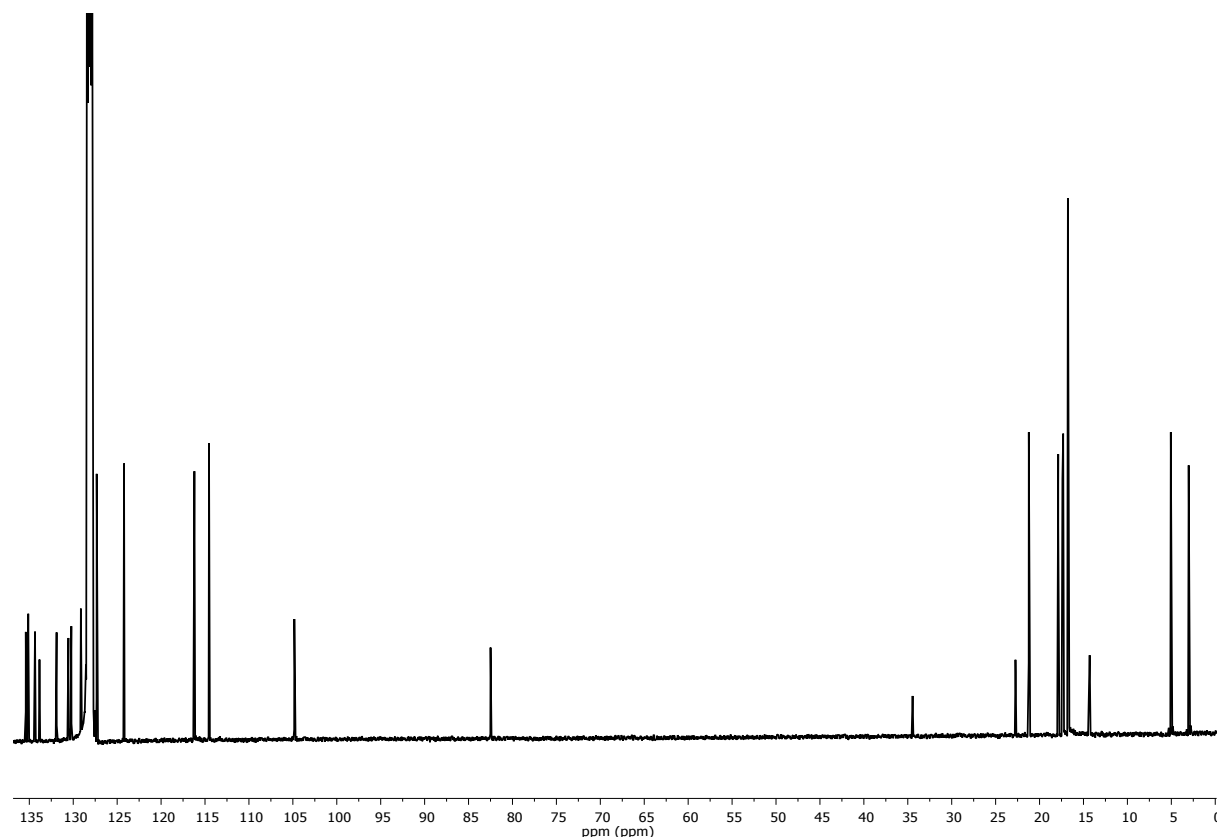


**Fig. S6.**  ${}^{13}\text{C}\{{}^1\text{H}\}$  NMR spectrum (benzene- $d_6$ , 125 MHz, 23 °C) of  $\text{Me}_2\text{SB}(\text{Cp},\text{I}^*)\text{ZrBr}_2$  (**2**).

$\text{Me}_2\text{SB}(\text{Cp}^{\text{Me}}, \text{I}^*)\text{ZrBr}_2$  (**3**)

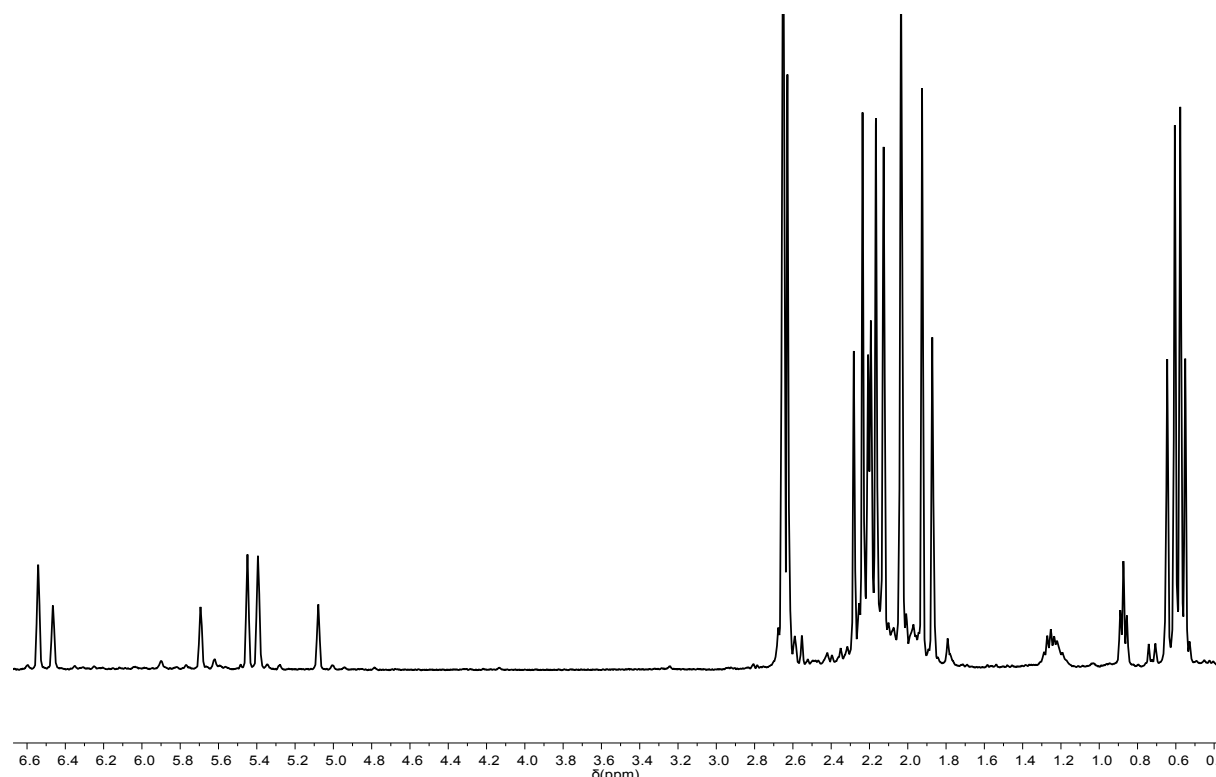


**Fig. S7.**  $^1\text{H}$  NMR spectrum (benzene- $d_6$ , 400 MHz, 23 °C) of  $\text{Me}_2\text{SB}(\text{Cp}^{\text{Me}}, \text{I}^*)\text{ZrBr}_2$  (**3**).

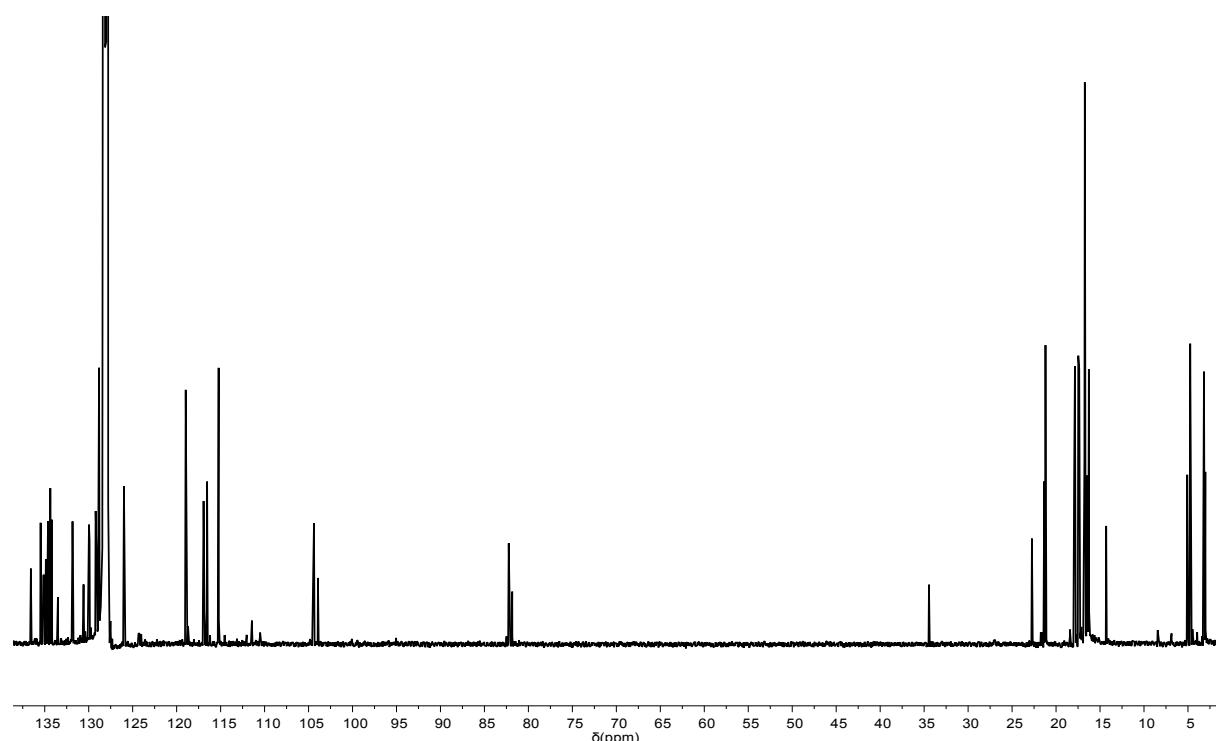


**Fig. S8.**  $^{13}\text{C}\{^1\text{H}\}$  NMR spectrum (benzene- $d_6$ , 125 MHz, 23 °C) of  $\text{Me}_2\text{SB}(\text{Cp}^{\text{Me}}, \text{I}^*)\text{ZrBr}_2$  (**3**).

$\text{Me}_2\text{SB}(\text{Cp},\text{I}^*)\text{Zr}(\text{CH}_2\text{Ph})_2$  (**4**)

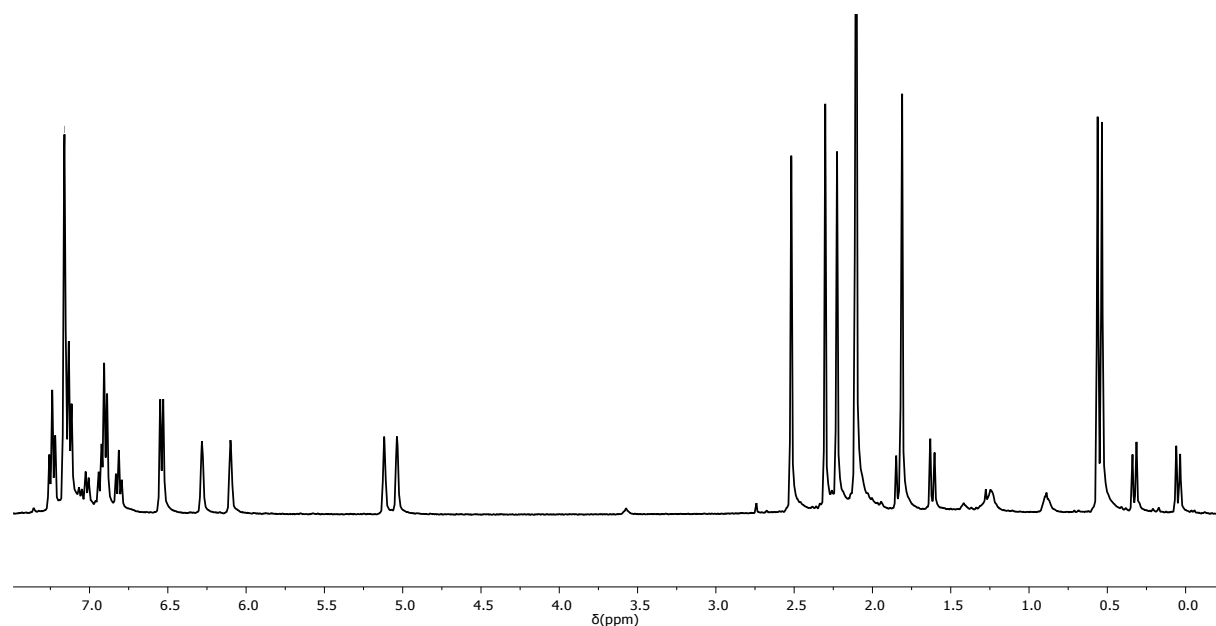


**Fig. S9.**  $^1\text{H}$  NMR spectrum (benzene- $d_6$ , 400 MHz, 23 °C) of  $\text{Me}_2\text{SB}(\text{Cp},\text{I}^*)\text{Zr}(\text{CH}_2\text{Ph})_2$  (**4**).

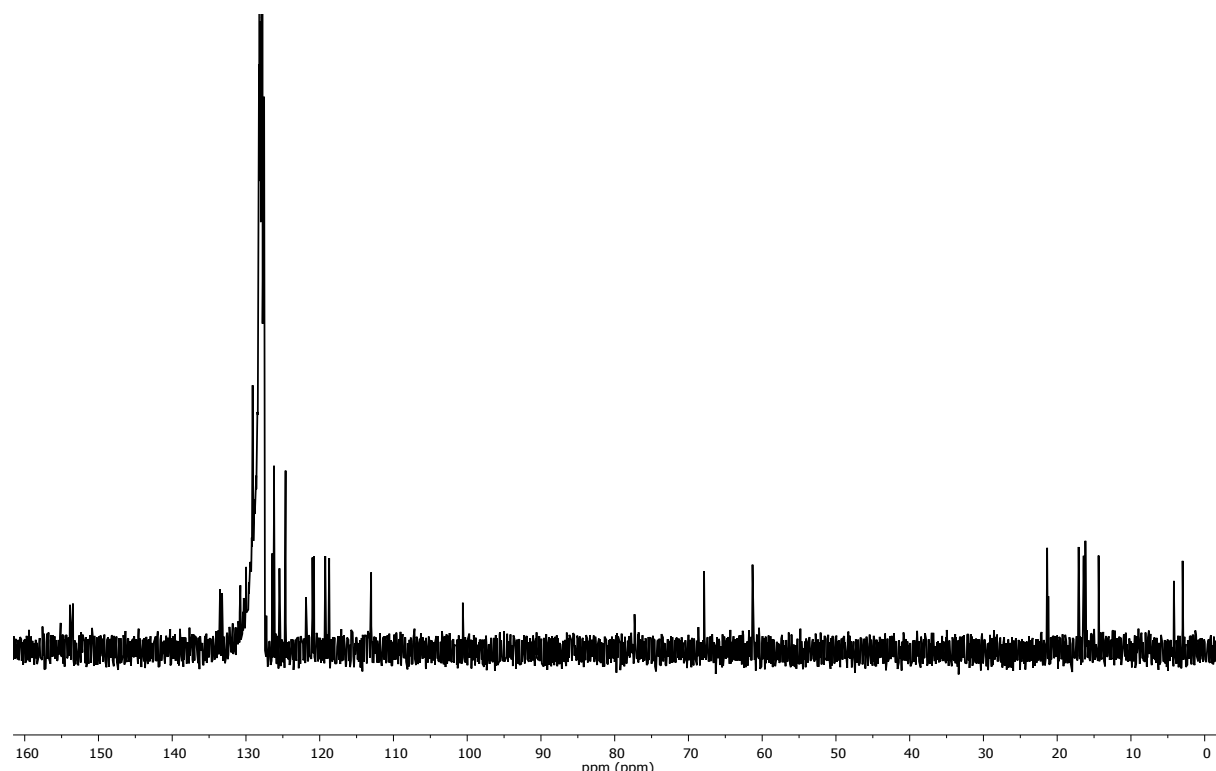


**Fig. S10.**  $^{13}\text{C}\{^1\text{H}\}$  NMR spectrum (benzene- $d_6$ , 125 MHz, 23 °C) of  $\text{Me}_2\text{SB}(\text{Cp},\text{I}^*)\text{Zr}(\text{CH}_2\text{Ph})_2$  (**4**).

$\text{Me}_2\text{SB}(\text{Cp}^{\text{Me}}, \text{I}^*)\text{Zr}(\text{CH}_2\text{Ph})_2$  (**5**)

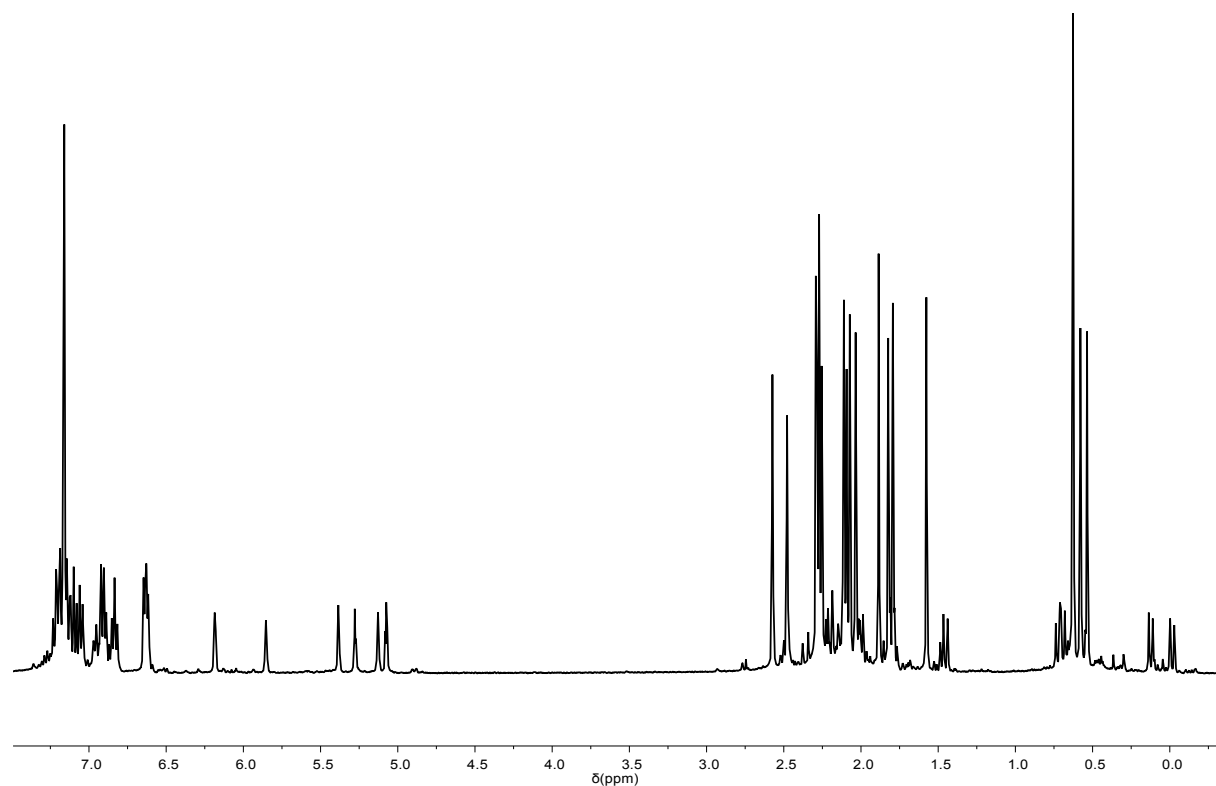


**Fig. S11.**  $^1\text{H}$  NMR spectrum (benzene- $d_6$ , 400 MHz, 23 °C) of  $\text{Me}_2\text{SB}(\text{Cp}^{\text{Me}}, \text{I}^*)\text{Zr}(\text{CH}_2\text{Ph})_2$  (**5**).

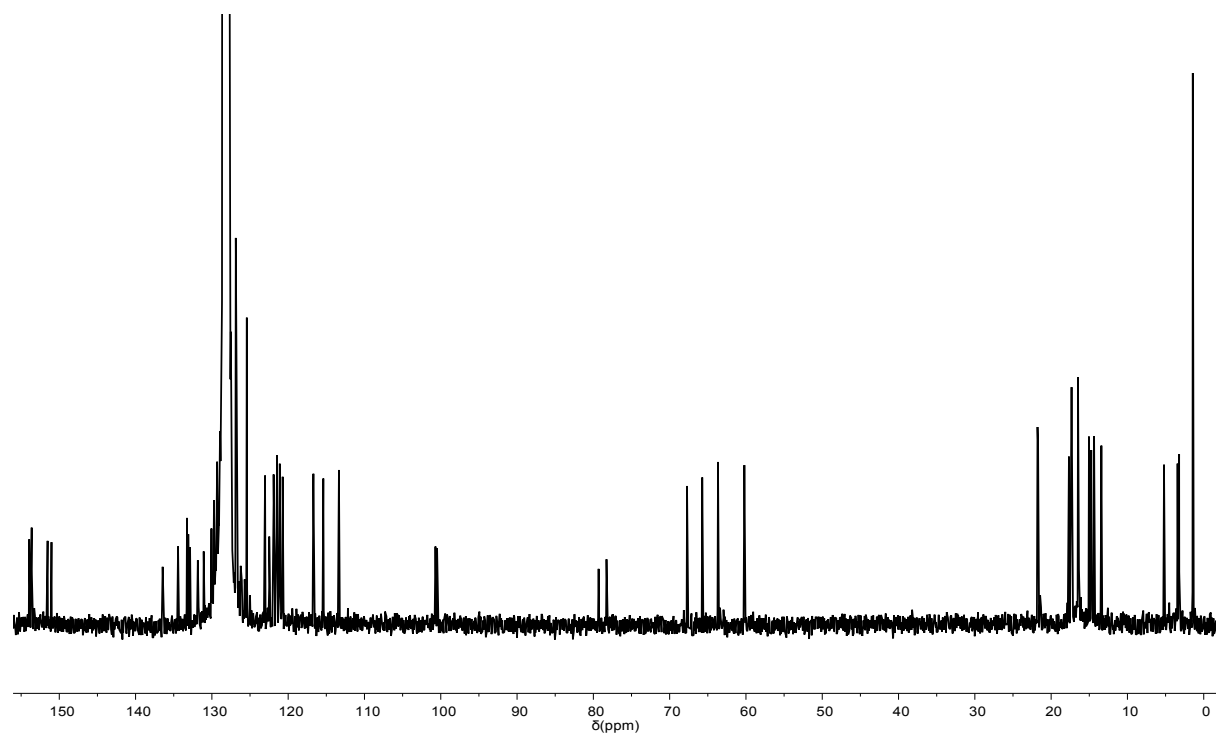


**Fig. S12.**  $^{13}\text{C}\{^1\text{H}\}$  NMR spectrum (benzene- $d_6$ , 125 MHz, 23 °C) of  $\text{Me}_2\text{SB}(\text{Cp}^{\text{Me}}, \text{I}^*)\text{Zr}(\text{CH}_2\text{Ph})_2$  (**5**).

$\text{Me}_2\text{SB}(\text{Cp},\text{I}^*)\text{ZrMe}_2$  (**6**)

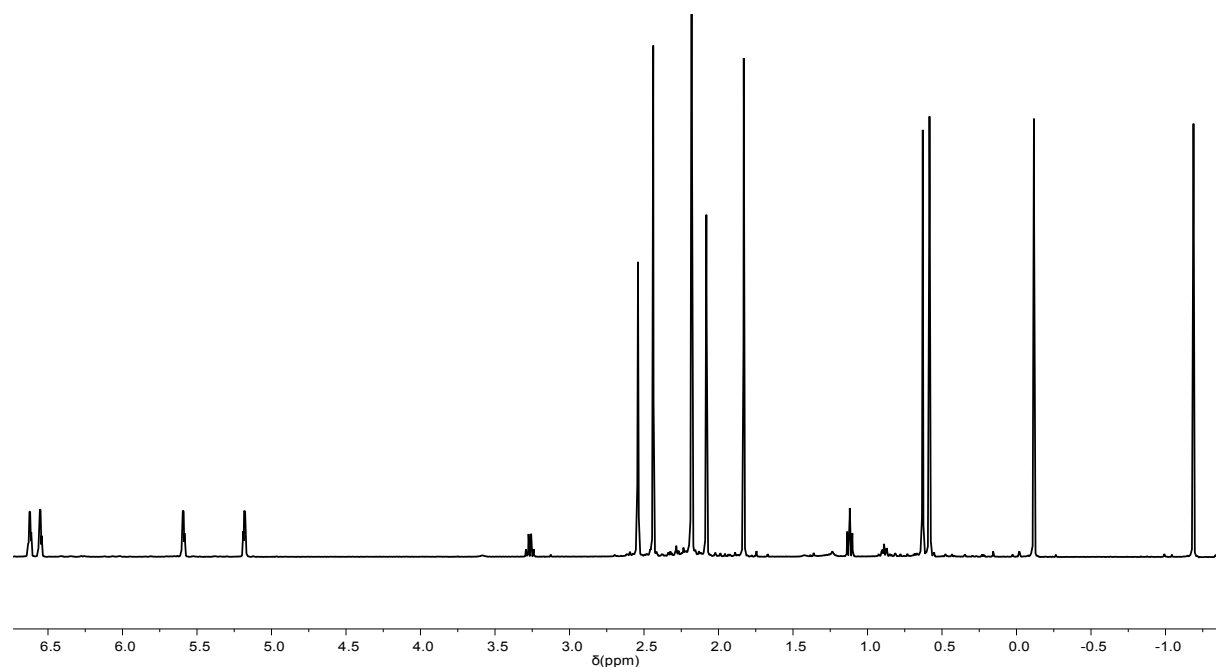


**Fig. S13.**  $^1\text{H}$  NMR spectrum (benzene- $d_6$ , 400 MHz, 23 °C) of  $\text{Me}_2\text{SB}(\text{Cp},\text{I}^*)\text{ZrMe}_2$  (**6**).

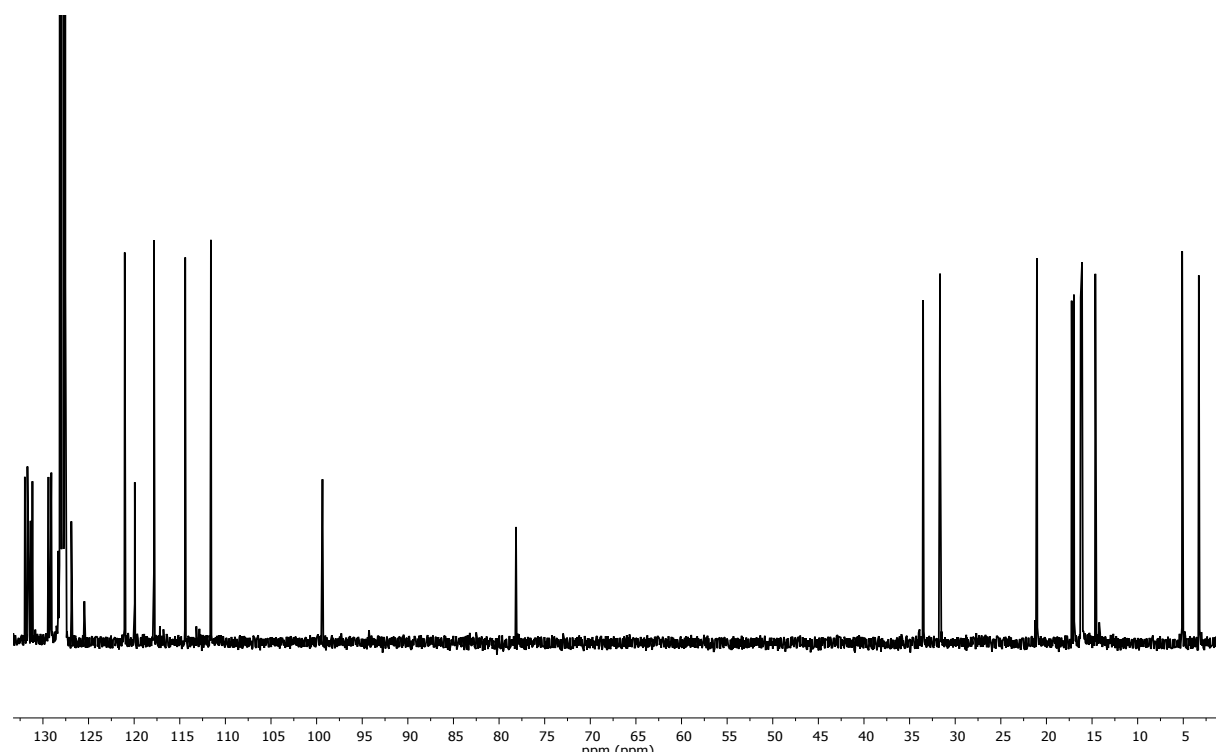


**Fig. S14.**  $^{13}\text{C}\{^1\text{H}\}$  NMR spectrum (benzene- $d_6$ , 125 MHz, 23 °C) of  $\text{Me}_2\text{SB}(\text{Cp},\text{I}^*)\text{ZrMe}_2$  (**6**).

$\text{Me}_2\text{SB}(\text{Cp}^{\text{Me}}, \text{I}^*)\text{ZrMe}_2$  (7)

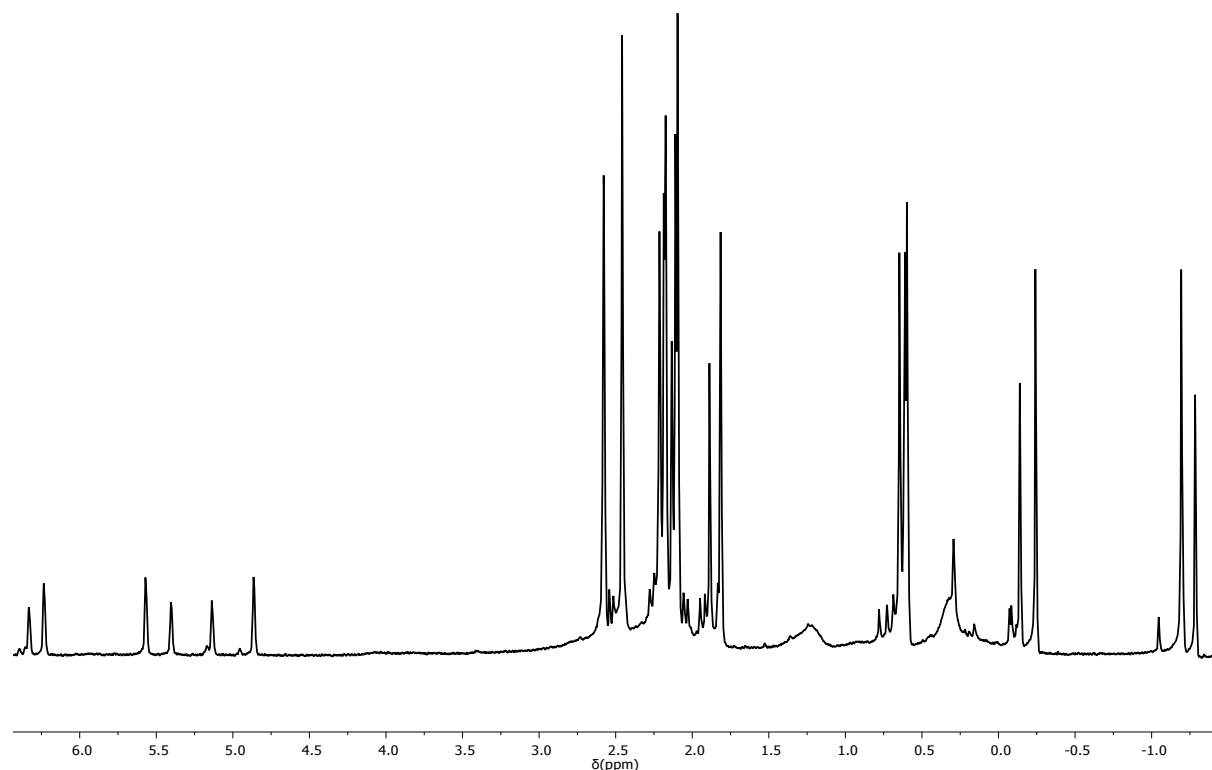


**Fig. S15.**  ${}^1\text{H}$  NMR spectrum (benzene- $d_6$ , 400 MHz, 23 °C) of  $\text{Me}_2\text{SB}(\text{Cp}^{\text{Me}}, \text{I}^*)\text{ZrMe}_2$  (7).

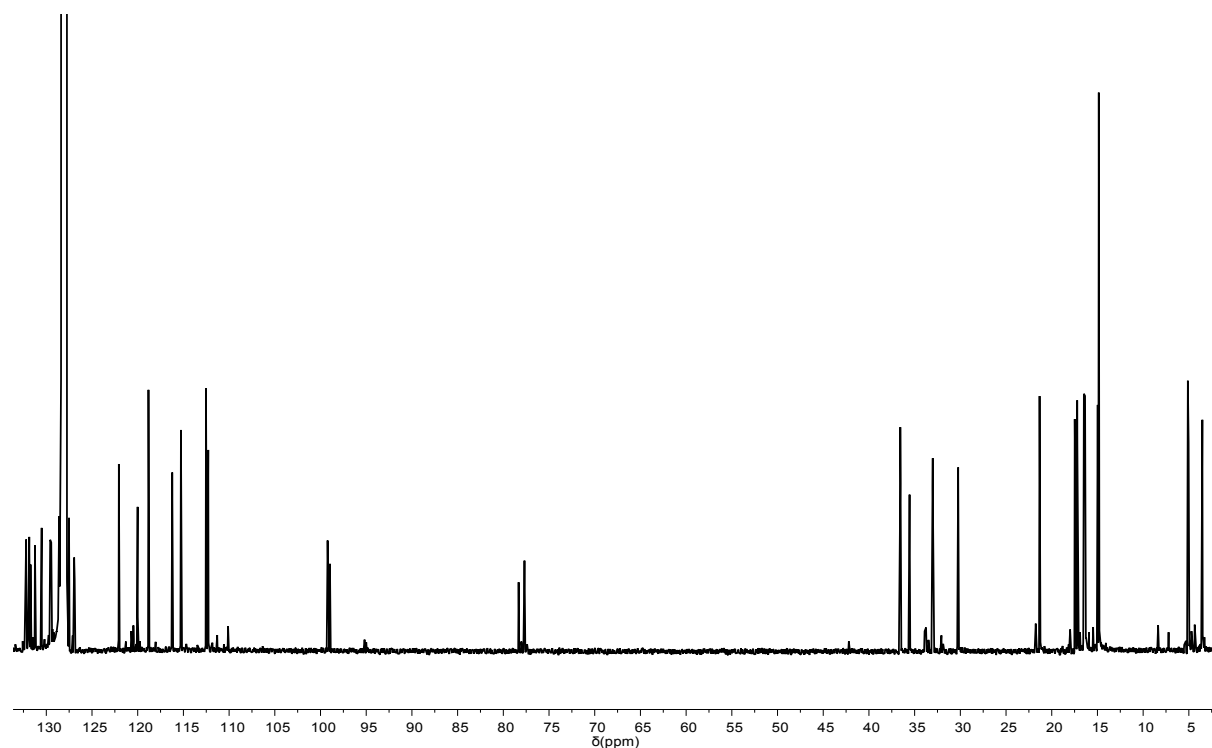


**Fig. S16.**  ${}^{13}\text{C}\{{}^1\text{H}\}$  NMR spectrum (benzene- $d_6$ , 125 MHz, 23 °C) of  $\text{Me}_2\text{SB}(\text{Cp}^{\text{Me}}, \text{I}^*)\text{ZrMe}_2$  (7).

**sMAO- $\text{Me}_2\text{SB}(\text{Cp},\text{I}^*)\text{ZrCl}_2$  ( $\mathbf{A}_{\text{sMAO}}$ )**

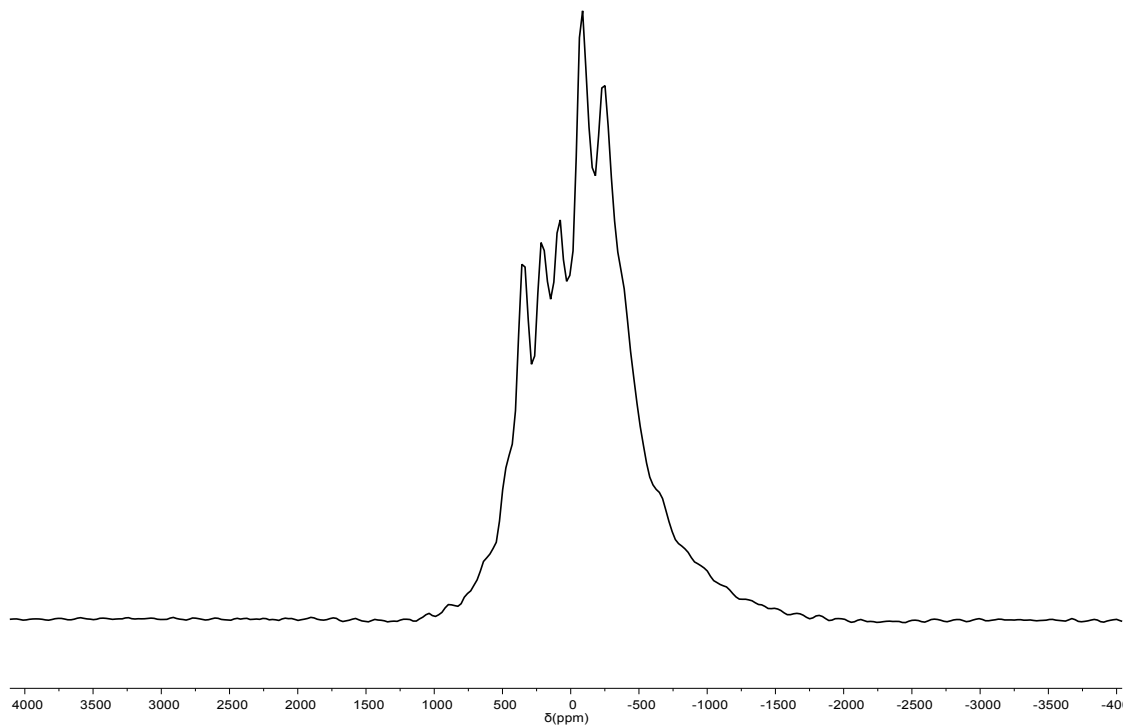


**Fig. S17.**  $^{27}\text{Al}$  DPMAS NMR spectrum (15 kHz, 23 °C) of sMAO- $\text{Me}_2\text{SB}(\text{Cp},\text{I}^*)\text{ZrCl}_2$  ( $\mathbf{A}_{\text{sMAO}}$ ).

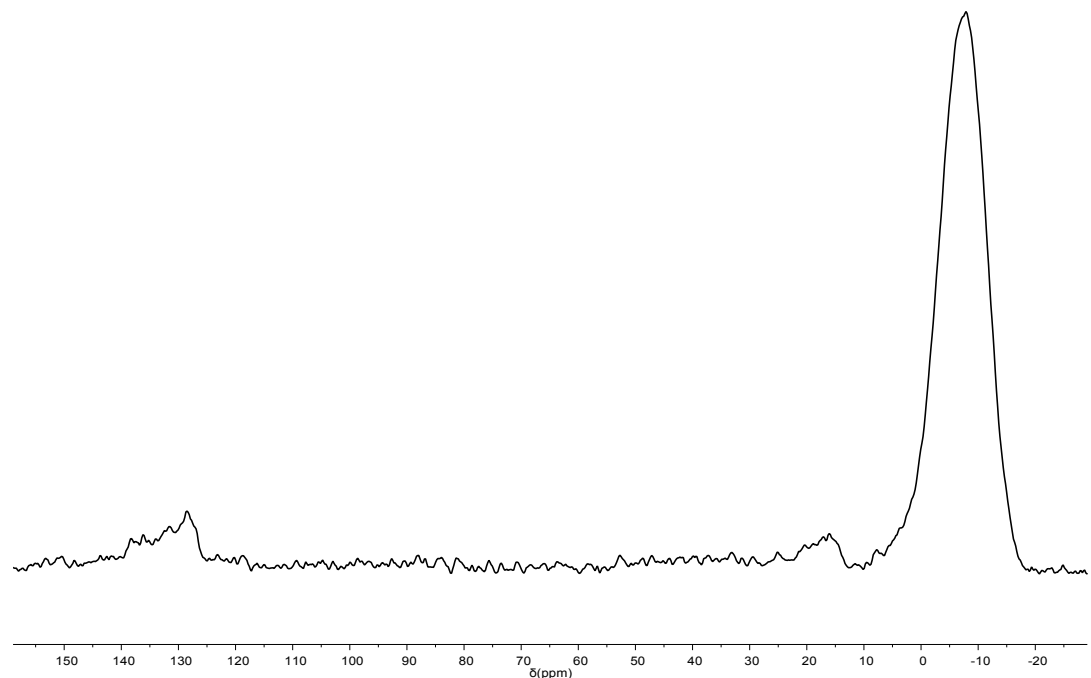


**Fig. S18.**  $^{13}\text{C}$  CPMAS NMR spectrum (10 kHz, 23 °C) of sMAO- $\text{Me}_2\text{SB}(\text{Cp},\text{I}^*)\text{ZrCl}_2$  ( $\mathbf{A}_{\text{sMAO}}$ ).

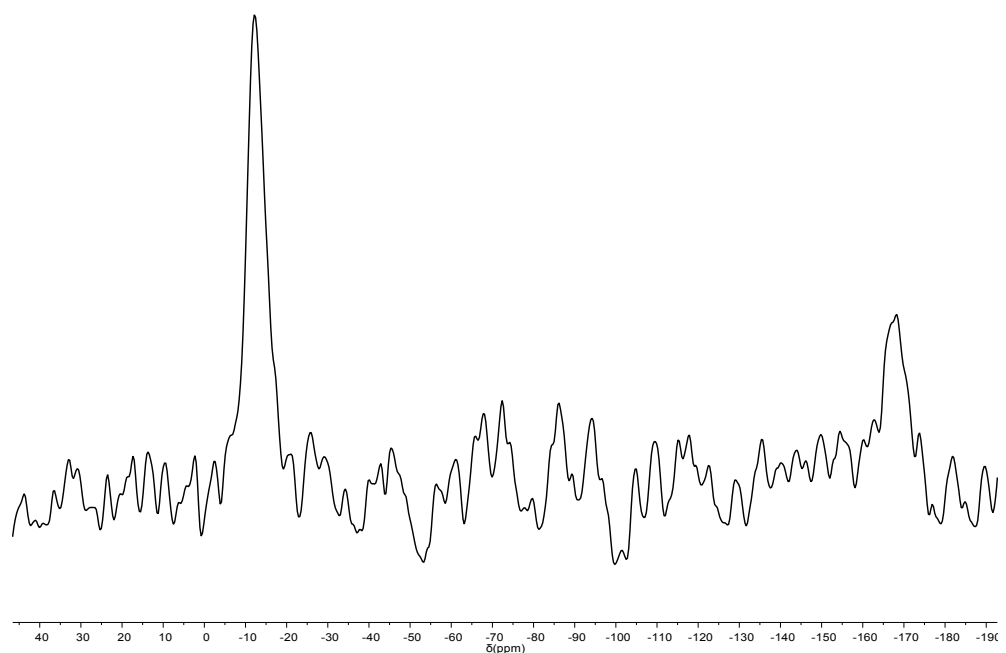


**Fig. S19.**  $^{29}\text{Si}$  CPMAS NMR spectrum (10 kHz, 23 °C) of sMAO- $\text{Me}_2\text{SB}(\text{Cp},\text{I}^*)\text{ZrCl}_2$  ( $\mathbf{A}_{\text{sMAO}}$ ).

**sMAO- $\text{Me}_2\text{SB}(\text{Cp},\text{I}^*)\text{Zr}(\text{CH}_2\text{Ph})_2$  ( $\mathbf{4}_{\text{sMAO}}$ )**

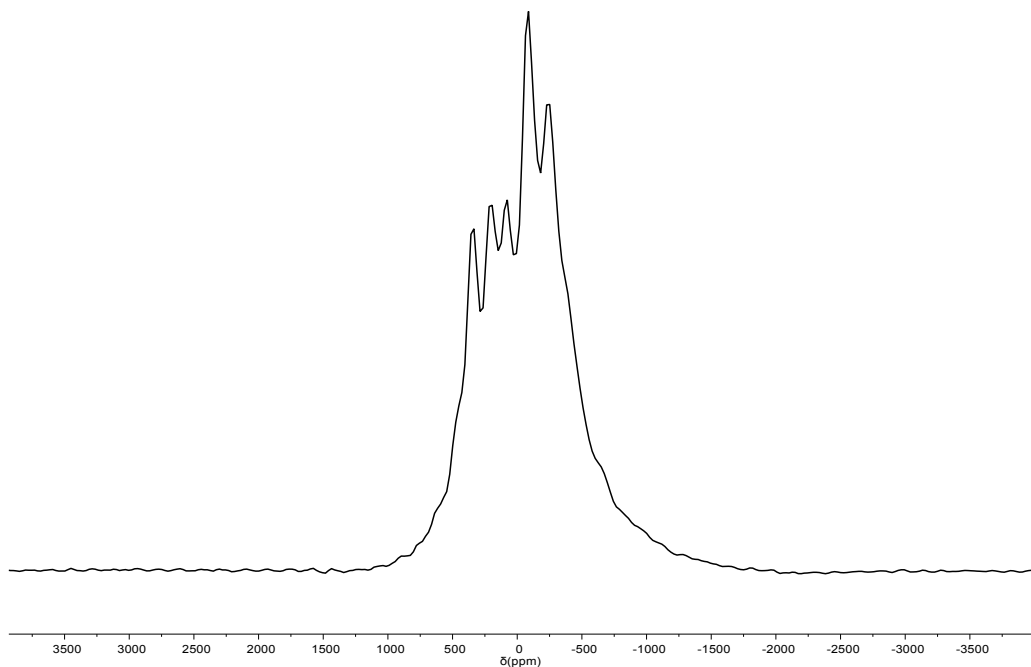


**Fig. S20.**  $^{27}\text{Al}$  DPMAS NMR spectrum (15 kHz, 23 °C) of sMAO- $\text{Me}_2\text{SB}(\text{Cp},\text{I}^*)\text{Zr}(\text{CH}_2\text{Ph})_2$  ( $\mathbf{4}_{\text{sMAO}}$ ).

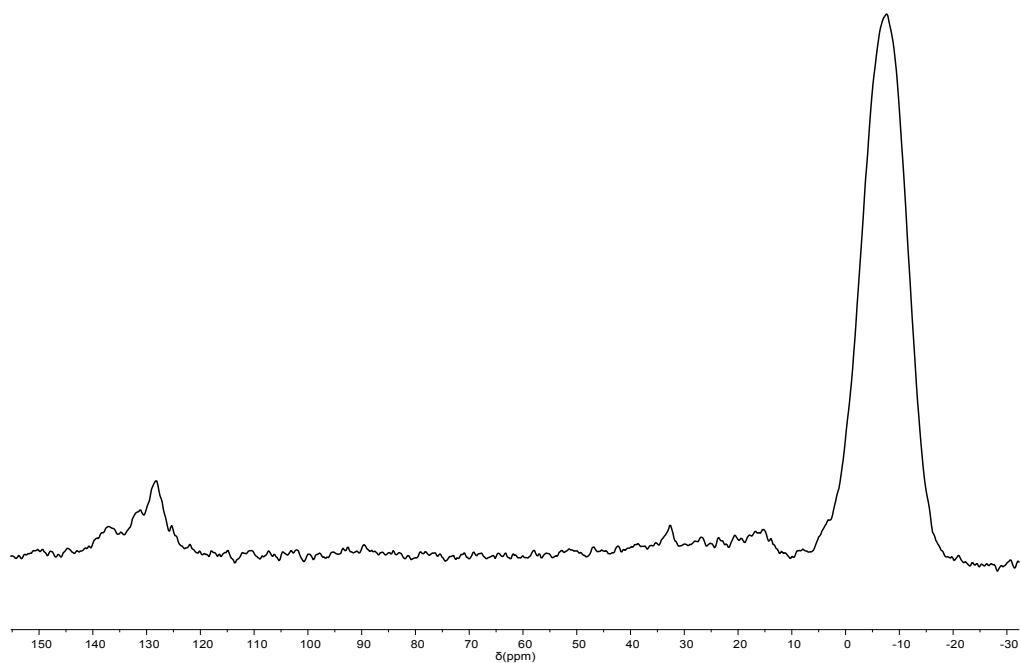


**Fig. S21.** <sup>13</sup>C CPMAS NMR spectrum (10 kHz, 23 °C) of sMAO-<sup>Me<sub>2</sub>SB(Cp,I<sup>\*</sup>)Zr(CH<sub>2</sub>Ph)<sub>2</sub></sup> (**4<sub>sMAO</sub>**).

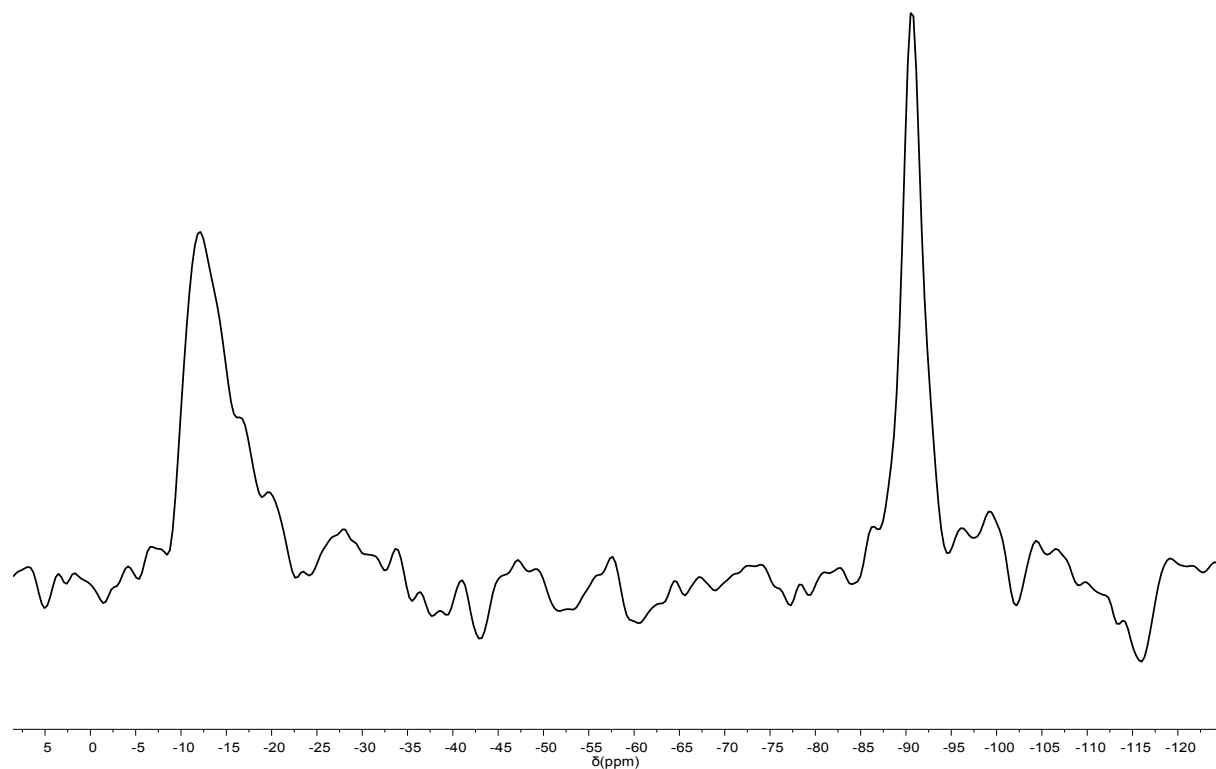


**Fig. S22.** <sup>29</sup>Si CPMAS NMR spectrum (10 kHz, 23 °C) of sMAO-<sup>Me<sub>2</sub>SB(Cp,I<sup>\*</sup>)Zr(CH<sub>2</sub>Ph)<sub>2</sub></sup> (**4<sub>sMAO</sub>**). The resonance at ~ -90.6 ppm corresponds to the signal from the probe.

**sMAO- $\text{Me}_2\text{SB}(\text{Cp},\text{I}^*)\text{ZrMe}_2$  ( $\mathbf{6}_{\text{sMAO}}$ )**

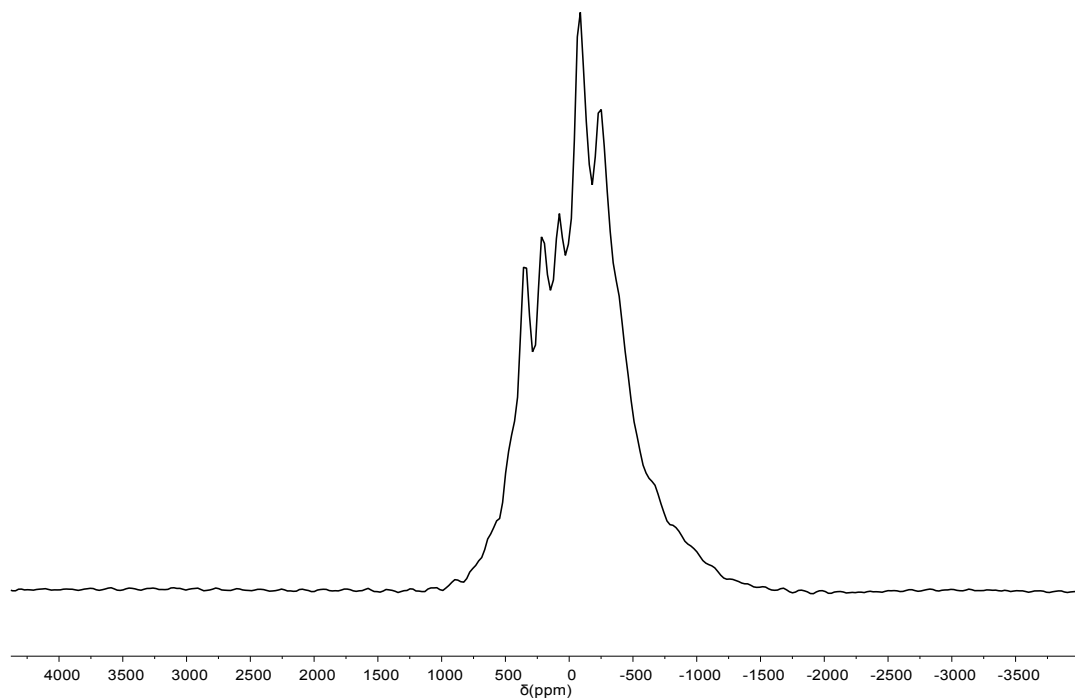


**Fig. S23.**  $^{27}\text{Al}$  DPMAS NMR spectrum (15 kHz, 23 °C) of sMAO- $\text{Me}_2\text{SB}(\text{Cp},\text{I}^*)\text{ZrMe}_2$  ( $\mathbf{6}_{\text{sMAO}}$ ).

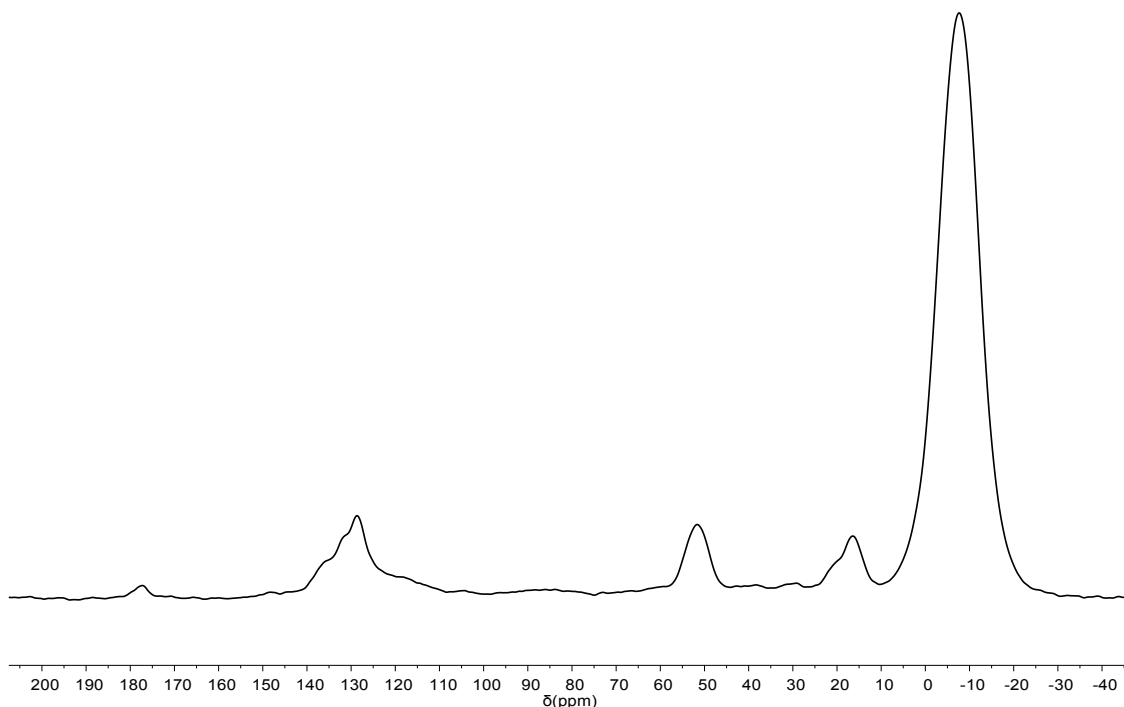


**Fig. S24.**  $^{13}\text{C}$  CPMAS NMR spectrum (10 kHz, 23 °C) of sMAO- $\text{Me}_2\text{SB}(\text{Cp},\text{I}^*)\text{ZrMe}_2$  ( $\mathbf{6}_{\text{sMAO}}$ ).

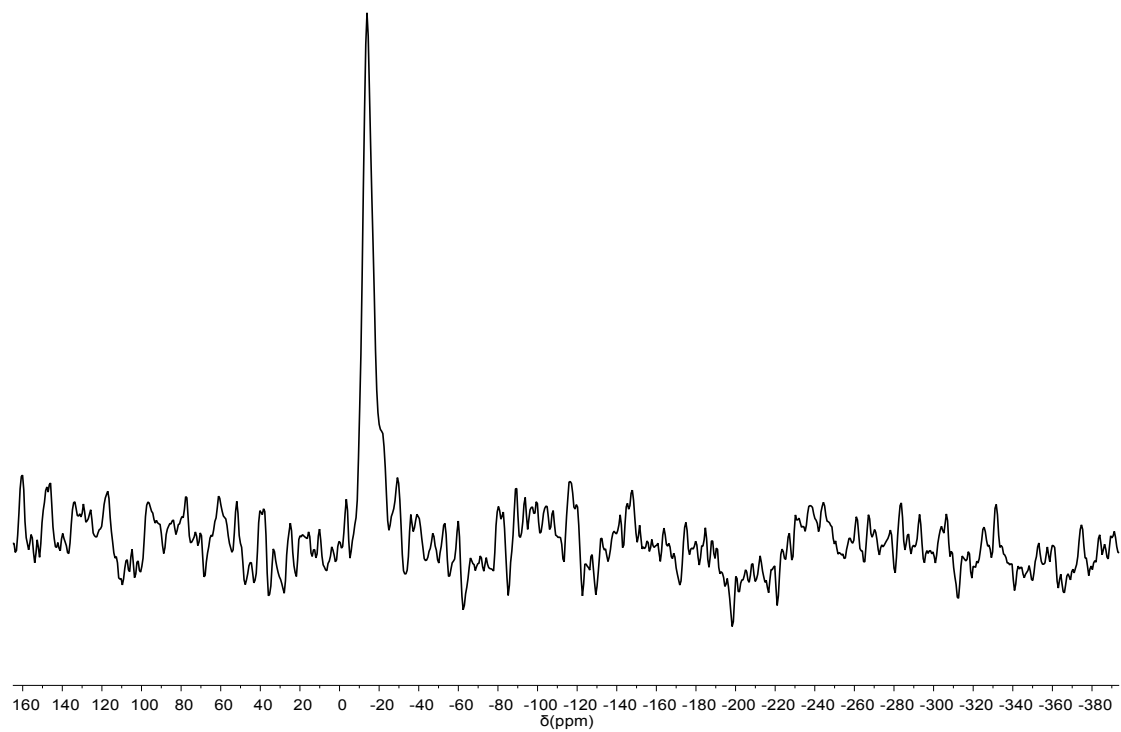


**Fig. S25.**  $^{29}\text{Si}$  CPMAS NMR spectrum (10 kHz, 23 °C) of sMAO- $\text{Me}_2\text{SB}(\text{Cp},\text{I}^*)\text{ZrMe}_2$  (**6<sub>sMAO</sub>**).

### 3. Additional Crystallographic Data

#### 3.1 Crystallographic details

Crystals were mounted on MiTeGen MicroMounts using perfluoropolyether oil and rapidly transferred to a goniometer head on a diffractometer fitted with an Oxford Cryosystems Cryostream open-flow nitrogen cooling device.<sup>1</sup> Data collections were carried out at 150 K using an Oxford Diffraction Supernova diffractometer using mirror-monochromated Cu  $K\alpha$  radiation ( $\lambda = 1.54178 \text{ \AA}$ ) and the data was processed using CrysAlisPro.<sup>2</sup> The structures were solved using direct methods (SIR-92)<sup>3</sup> or a charge flipping algorithm (SUPERFLIP)<sup>4</sup> and refined by full-matrix least-squares procedures using the Win-GX software suite.<sup>5</sup>

#### 3.2 Geometric parameters and numbering scheme

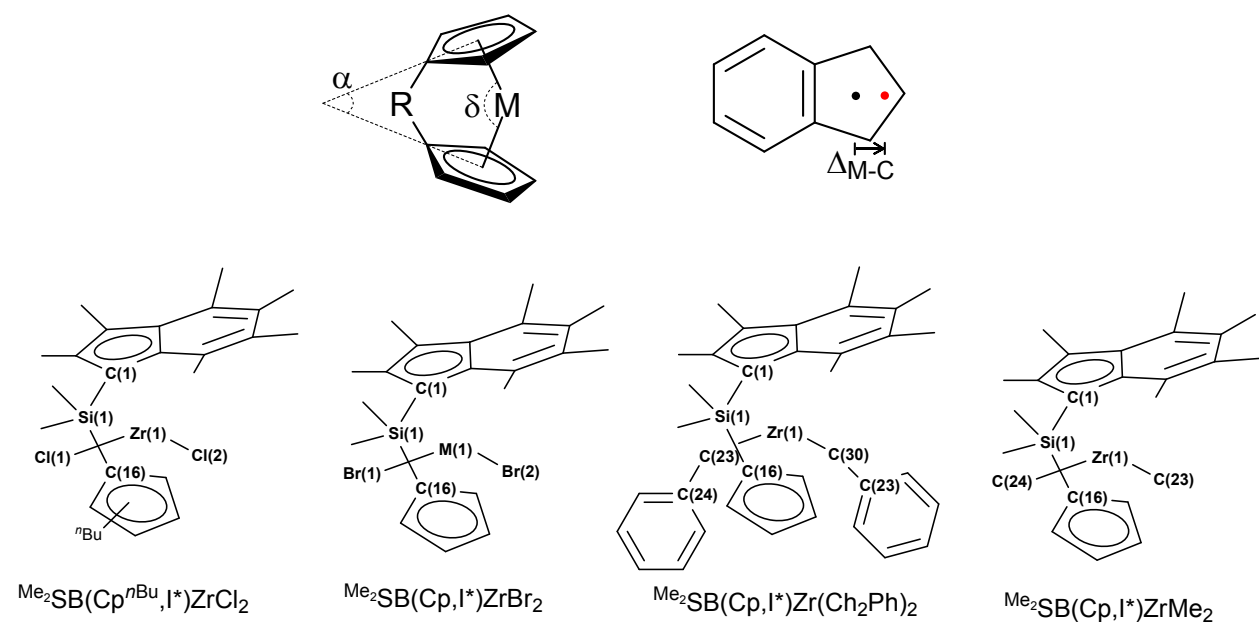


**Fig. S26.** Geometric parameters and numbering scheme

### 3.3. Experimental crystallographic data

**Table S1.** Selected crystallographic data **E-1, Z-1, 2, 4** and **6**.

	<b>E-1</b>	<b>Z-1</b>	<b>2</b>	<b>4</b>	<b>6</b>
Zr(1)-Ind* <sub>cent</sub>	2.2308(1)	2.2200(1)	2.2300(1)	2.2615(1)	2.2442(1)
Zr(1)-Cp <sup>R</sup> <sub>cent</sub>	2.2011(1)	2.2143(1)	2.2012(1)	2.1943(1)	2.2201(1)
Zr(1)-X(1)	2.4340(4)	2.4262(4)	2.6067(5)	-	-
Zr(1)-X(2)	2.4433(4)	2.4327(4)	2.5856(5)	-	-
Zr(1)-C(23)	-	-	-	2.293(10)	2.269(2)
Zr(1)-C(30)	-	-	-	2.314(10)	-
Zr(1)-C(24)	-	-	-	-	2.280(2)
Si(1)-C(1)	1.8981(16)	1.8999(16)	Si(1)-C(1)	1.917(11)	1.898(2)
Si(1)-C(16)	1.8749(17)	1.8804(17)	Si(1)-C(16)	1.868(12)	1.866(3)
Δ <sub>M-C</sub>	0.019	0.018	0.061	0.064	0.063
α	60.20	60.25	60.14	59.80	59.16
δ	127.49(1)	126.98(1)	126.32(1)	126.88(1)	126.96(1)
X(1)-Zr(1)-X(2)	96.892(16)	97.130(17)	96.664(18)	-	-
C(23)-Zr(1)-C(30)	-	-	-	96.6(4)	-
C(23)-Zr(1)-C(24)	-	-	-	-	97.60(11)
Zr(1)-C(23)-C(24)	-	-	-	123.6(3)	-
Zr(1)-C(30)-C(31)	-	-	-	126.9(3)	-
C(1)-Si(1)-C(16)	94.76(7)	95.13(7)	94.19(17)	96.5(2)	96.65(10)

**Table S2.** Selected experimental crystallographic data for complexes **E-1**, **Z-1**, **2**, **4** and **6**.

Complex	<b>E-1</b>	<b>Z-1</b>	<b>2</b>	<b>4</b>	<b>6</b>
<b>Crystal data</b>					
Chemical formula	C <sub>26</sub> H <sub>36</sub> Cl <sub>2</sub> SiZr	C <sub>26</sub> H <sub>36</sub> Cl <sub>2</sub> SiZr	C <sub>22</sub> H <sub>28</sub> Br <sub>2</sub> SiZr	C <sub>36</sub> H <sub>42</sub> SiZr	C <sub>24</sub> H <sub>34</sub> SiZr
M <sub>r</sub>	538.76	538.76	571.57	594.00	441.82
Crystal system, space group	Monoclinic, <i>P2<sub>1</sub>/n</i>	Triclinic, <i>P1</i>	Orthorhombic, <i>Fdd2</i>	Triclinic, <i>P1</i>	Orthorhombic, <i>Fdd2</i>
Temperature (K)	150	150	150	150	150
a, b, c (Å)	11.6286 (1), 14.8501 (1), 14.9589 (1)	8.7586 (2), 11.3702 (3), 14.6917 (4)	52.0095 (12), 19.2685 (5), 8.6866 (2)	12.4776 (6), 14.8663 (12), 17.9117 (5)	52.1310 (14), 19.3460 (5), 8.7251 (3)
α, β, γ (°)	90, 99.332 (1), 90	104.583 (2), 94.052 (2), 103.622 (2)	90, 90, 90	100.463 (5), 101.218 (4), 105.208 (6)	90, 90, 90
V (Å <sup>3</sup> )	2549.00 (3)	1362.94 (6)	8705.2 (4)	3048.5 (3)	8799.5 (4)
Z	4	2	16	4	16
Radiation type	Cu Kα	Cu Kα	Cu Kα	Cu Kα	Cu Kα
μ (mm <sup>-1</sup> )	5.98	5.59	8.98	3.48	4.63
Crystal size (mm)	0.26 × 0.10 × 0.08	0.28 × 0.15 × 0.03	0.16 × 0.08 × 0.05	0.11 × 0.08 × 0.03	0.24 × 0.12 × 0.04
<b>Data Collection</b>					
Diffractometer	SuperNova, Dual, Cu at home/near, Atlas diffractometer	SuperNova, Dual, Cu at zero, Atlas diffractometer	SuperNova, Dual, Cu at zero, Atlas diffractometer	SuperNova, Dual, Cu at zero, Atlas diffractometer	SuperNova, Dual, Cu at zero, Atlas diffractometer

Absorption correction	Gaussian CrysAlisPro 1.171.39.46 (Rigaku Oxford Diffraction, 2018) Numerical absorption correction based on gaussian integration over a multifaceted crystal model Empirical absorption correction using spherical harmonics, implemented in SCALE3 ABSPACK scaling algorithm.	Multi-scan CrysAlisPro 1.171.38.41 (Rigaku Oxford Diffraction, 2015) Empirical absorption correction using spherical harmonics, implemented in SCALE3 ABSPACK scaling algorithm.	Multi-scan CrysAlisPro 1.171.38.41 (Rigaku Oxford Diffraction, 2015) Empirical absorption correction using spherical harmonics, implemented in SCALE3 ABSPACK scaling algorithm.	Multi-scan CrysAlisPro 1.171.38.41 (Rigaku Oxford Diffraction, 2015) Empirical absorption correction using spherical harmonics, implemented in SCALE3 ABSPACK scaling algorithm.	Gaussian CrysAlisPro 1.171.38.43b (Rigaku Oxford Diffraction, 2015) Numerical absorption correction based on gaussian integration over a multifaceted crystal model Empirical absorption correction using spherical harmonics, implemented in SCALE3 ABSPACK scaling algorithm.
$T_{\min}$ , $T_{\max}$	0.510, 1.000	0.579, 1.000	0.744, 1.000	0.787, 1.000	0.498, 1.000
No. of measured, independent and observed [ $I > 2\sigma(I)$ ] reflections	51024, 5221, 4848	27786, 5566, 5170	19282, 4436, 4388	19991, 19991, 14258	42887, 4497, 4471
$R_{\text{int}}$	0.030	0.033	0.038		0.037
<b>Refinement</b>					
$R[F^2 > 2\sigma(F^2)]$ , $wR(F^2)$ , $S$	0.021, 0.055, 1.03	0.022, 0.056, 1.05	0.023, 0.058, 1.03	0.152, 0.371, 1.48	0.018, 0.042, 1.05
No. of reflections	5221	5566	4436	19991	4497
No. of parameters	280	280	244	696	246

No. of restraints	0	0	1	21	1
$(\Delta/\sigma)_{\max}$					
$\Delta\rho_{\max}, \Delta\rho_{\min}$ (e Å <sup>-3</sup> )	0.53, -0.31	0.41, -0.45	0.43, -0.40	13.47, -2.22	0.25, -0.22

Computer programs: CrysAlisPro 1.171.39.46 (Rigaku OD, 2018), CrysAlisPro 1.171.38.41 (Rigaku OD, 2015), SUPERFLIP Palatinus, L.; Chapuis, G. J. Appl. Cryst. 2007, 40, 786-790., SIR92 Altomare, A.; Cascarano, G.; Giacovazzo, C.; Guagliardi, A. J. Appl. Cryst. 1994, 27, 435., SUPERFLIP. Palatinus, L.; Chapuis, G. J. Appl. Cryst. 2007, 40, 786-790., SHEXL2014 (Sheldrick, 2014), ORTEP-3 for Windows. Farrugia, L. J. J. Appl. Cryst. 1997, 30, 565...

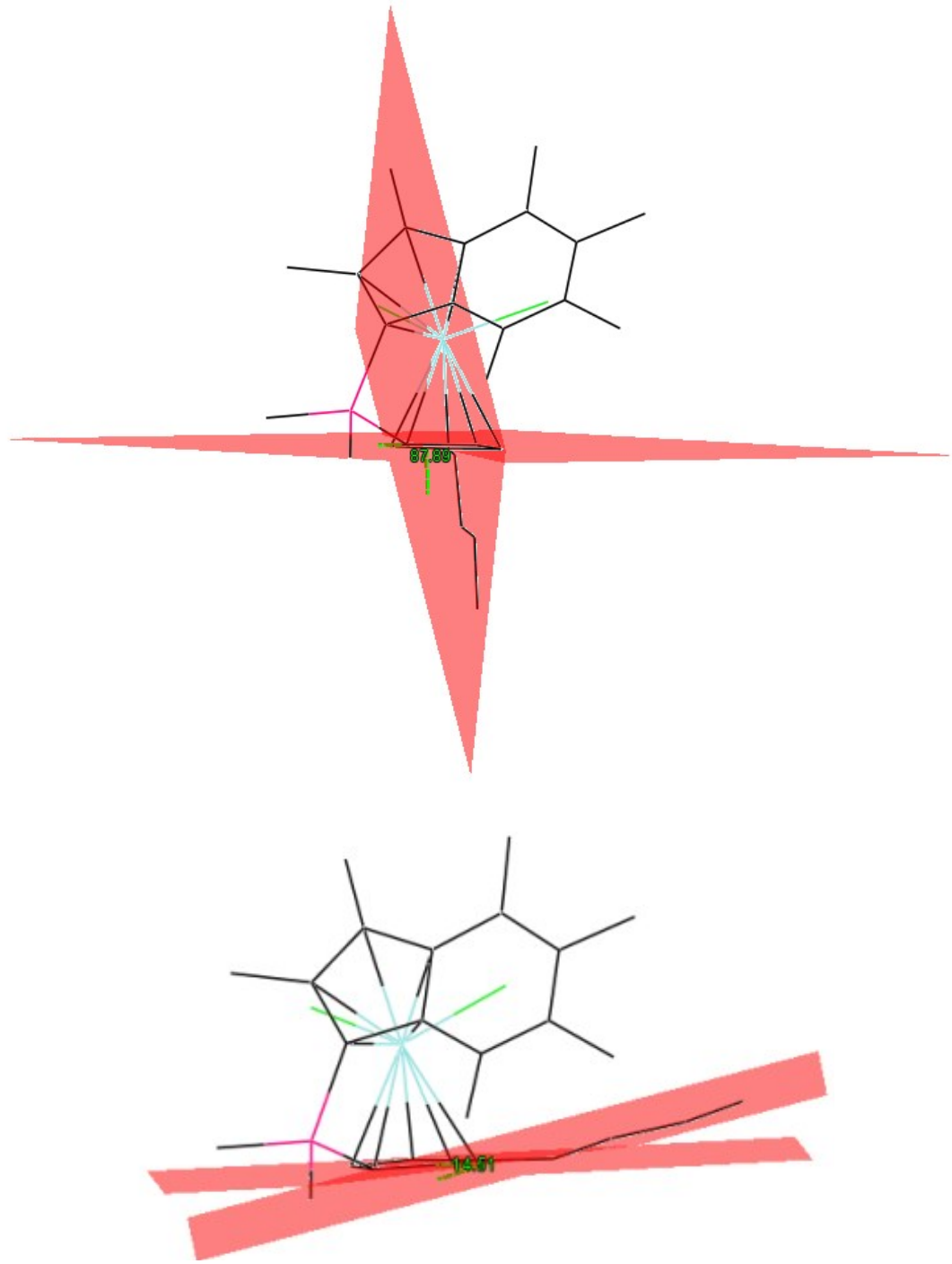


**Fig. S27.** Depiction of the angle between the plane of the Cp ring and *n*-butyl chain of *E*-Me<sub>2</sub>SB(Cp<sup>n</sup>Bu,I\*)ZrCl<sub>2</sub> (**E-1**) (top) and *E*-Me<sub>2</sub>SB(Cp<sup>n</sup>Bu,I\*)ZrCl<sub>2</sub> (**Z-1**) (bottom).

#### 4. Additional polymerisation data

##### 4.1 Polymerisation activities and molecular weights tables

**Table S3.** Slurry-phase ethylene polymerisation with sMAO- $\text{Me}_2\text{SB}(\text{Cp},\text{I}^*)\text{ZrCl}_2$  ( $\mathbf{A}_{\text{sMAO}}$ )

Catalyst	[Al] <sub>0</sub> / [Zr] <sub>0</sub>	Temperature (°C)	Time (minutes)	Activity (kg <sub>PE</sub> mol <sub>Zr</sub> <sup>-1</sup> h <sup>-1</sup> bar <sup>-1</sup> )	$M_w$ (kg mol <sup>-1</sup> )	$M_w/M_n$
$\mathbf{A}_{\text{sMAO}}$	300	50	30	10035 ± 902	177	4.2
$\mathbf{A}_{\text{sMAO}}$	300	60	30	10784 ± 421	108	3.5
$\mathbf{A}_{\text{sMAO}}$	300	70	30	9653 ± 275	90	3.7
$\mathbf{A}_{\text{sMAO}}$	300	80	30	8154 ± 535	72	4.4
$\mathbf{A}_{\text{sMAO}}$	300	90	30	6140 ± 403	68	3.2
$\mathbf{A}_{\text{sMAO}}$	200	50	30	6794 ± 705	192	2.8
$\mathbf{A}_{\text{sMAO}}$	200	60	30	7075 ± 326	140	3.2
$\mathbf{A}_{\text{sMAO}}$	200	70	30	6081 ± 8	104	3.0
$\mathbf{A}_{\text{sMAO}}$	200	80	30	5143 ± 129	76	3.3
$\mathbf{A}_{\text{sMAO}}$	200	90	30	3710 ± 407	65	2.8
$\mathbf{A}_{\text{sMAO}}$	200	80	5	10066 ± 1053	123	3.9
$\mathbf{A}_{\text{sMAO}}$	200	80	15	6229 ± 11	98	3.9
$\mathbf{A}_{\text{sMAO}}$	200	80	60	4967 ± 294	65	3.2
$\mathbf{A}_{\text{sMAO}}$	150	50	30	5999 ± 646	159	4.0
$\mathbf{A}_{\text{sMAO}}$	150	60	30	6318 ± 497	137	3.8
$\mathbf{A}_{\text{sMAO}}$	150	70	30	5845 ± 15	88	3.5
$\mathbf{A}_{\text{sMAO}}$	150	80	30	4940 ± 45	74	3.7
$\mathbf{A}_{\text{sMAO}}$	150	90	30	3394 ± 232	51	3.5
$\mathbf{A}_{\text{sMAO}}$	100	50	30	4175 ± 28	163	3.3
$\mathbf{A}_{\text{sMAO}}$	100	60	30	4022 ± 30	131	3.7
$\mathbf{A}_{\text{sMAO}}$	100	70	30	3737 ± 301	89	3.6
$\mathbf{A}_{\text{sMAO}}$	100	80	30	3049 ± 347	62	3.8
$\mathbf{A}_{\text{sMAO}}$	100	90	30	2117 ± 82	47	2.9

Polymerisation conditions: 150 mg TiBA scavenger, 2 bar ethylene, 10 mg pre-catalyst, 50 mL hexane.

**Table S4.** Slurry-phase ethylene polymerisation with sMAO- $\text{Me}_2\text{SB}(\text{Cp}^{\text{Me}}, \text{I}^*)\text{ZrCl}_2$  (**B<sub>sMAO</sub>**)

Catalyst	Temperature (°C)	Time (minutes)	Activity (kg <sub>PE</sub> mol <sub>Zr</sub> <sup>-1</sup> h <sup>-1</sup> bar <sup>-1</sup> )	$M_w$ (kg mol <sup>-1</sup> )	$M_w/M_n$
<b>B<sub>sMAO</sub></b>	50	30	4030 ± 6	197	2.8
<b>B<sub>sMAO</sub></b>	60	30	4223 ± 219	144	2.7
<b>B<sub>sMAO</sub></b>	70	30	4531 ± 328	120	2.7
<b>B<sub>sMAO</sub></b>	80	30	4560 ± 58	81	3.0
<b>B<sub>sMAO</sub></b>	90	30	3870 ± 158	75	2.7
<b>B<sub>sMAO</sub></b>	80	5	5715 ± 361	-	-
<b>B<sub>sMAO</sub></b>	80	15	5207 ± 39	-	-
<b>B<sub>sMAO</sub></b>	80	60	3814 ± 250	-	-

Polymerisation conditions:  $[\text{Al}]_0:[\text{Zr}]_0 = 200:1$ , 150 mg TiBA scavenger, 2 bar ethylene, 10 mg pre-catalyst, 50 mL hexane.

**Table S5.** Slurry-phase ethylene polymerisation with sMAO-Z- $\text{Me}_2\text{SB}(\text{Cp}^{n\text{Bu}}, \text{I}^*)\text{ZrCl}_2$  (**Z-1<sub>sMAO</sub>**)

Catalyst	Temperature (°C)	Time (minutes)	Activity (kg <sub>PE</sub> mol <sub>M</sub> <sup>-1</sup> h <sup>-1</sup> bar <sup>-1</sup> )	$M_w$ (kg mol <sup>-1</sup> )	$M_w/M_n$
<b>Z-1<sub>sMAO</sub></b>	50	30	6142 ± 87	138	3.1
<b>Z-1<sub>sMAO</sub></b>	60	30	5484 ± 196	116	3.0
<b>Z-1<sub>sMAO</sub></b>	70	30	5391 ± 182	94	2.9
<b>Z-1<sub>sMAO</sub></b>	80	30	4330 ± 122	80	3.2
<b>Z-1<sub>sMAO</sub></b>	90	30	3101 ± 177	62	3.2

Polymerisation conditions:  $[\text{Al}]_0:[\text{Zr}]_0 = 200:1$ , 150 mg TiBA scavenger, 2 bar ethylene, 10 mg pre-catalyst, 50 mL hexane.

**Table S6.** Slurry-phase ethylene polymerisation with sMAO-*E*-Me<sub>2</sub>SB(Cp<sup>nBu</sup>,I\*)ZrCl<sub>2</sub> (***E*-1<sub>sMAO</sub>**)

Catalyst	Temperature (°C)	Time (minutes)	Activity (kg <sub>PE</sub> mol <sub>Zr</sub> <sup>-1</sup> h <sup>-1</sup> bar <sup>-1</sup> )	M <sub>w</sub> (kg mol <sup>-1</sup> )	M <sub>w</sub> /M <sub>n</sub>
<b><i>E</i>-1<sub>sMAO</sub></b>	50	30	6638 ± 224	95	3.0
<b><i>E</i>-1<sub>sMAO</sub></b>	60	30	7036 ± 23	78	2.8
<b><i>E</i>-1<sub>sMAO</sub></b>	70	30	6481 ± 281	68	3.1
<b><i>E</i>-1<sub>sMAO</sub></b>	80	30	5553 ± 344	56	3.1
<b><i>E</i>-1<sub>sMAO</sub></b>	90	30	4467 ± 159	46	3.5

Polymerisation conditions: [Al]<sub>0</sub>:[Zr]<sub>0</sub> = 200:1, 150 mg TiBA scavenger, 2 bar ethylene, 10 mg pre-catalyst, 50 mL hexane.

**Table S7.** Slurry-phase ethylene polymerisation with sMAO-Me<sub>2</sub>SB(Cp,I\*)ZrBr<sub>2</sub> (**2<sub>sMAO</sub>**)

Catalyst	Temperature (°C)	Time (minutes)	Activity (kg <sub>PE</sub> mol <sub>Zr</sub> <sup>-1</sup> h <sup>-1</sup> bar <sup>-1</sup> )	M <sub>w</sub> (kg mol <sup>-1</sup> )	M <sub>w</sub> /M <sub>n</sub>
<b>2<sub>sMAO</sub></b>	50	30	6668 ± 606	190	3.3
<b>2<sub>sMAO</sub></b>	60	30	6408 ± 4	137	3.3
<b>2<sub>sMAO</sub></b>	70	30	5733 ± 128	98	3.5
<b>2<sub>sMAO</sub></b>	80	30	4588 ± 244	63	3.2
<b>2<sub>sMAO</sub></b>	90	30	3611 ± 132	66	3.6
<b>2<sub>sMAO</sub></b>	80	5	7529 ± 371	-	-
<b>2<sub>sMAO</sub></b>	80	15	5446 ± 241	-	-
<b>2<sub>sMAO</sub></b>	80	60	3657 ± 19	-	-

Polymerisation conditions: [Al]<sub>0</sub>:[Zr]<sub>0</sub> = 200:1, 150 mg TiBA scavenger, 2 bar ethylene, 10 mg pre-catalyst, 50 mL hexane.

**Table S8.** Slurry-phase ethylene polymerisation with sMAO-<sup>Me<sub>2</sub></sup>SB(Cp<sup>Me</sup>,I\*)ZrBr<sub>2</sub> (**3<sub>sMAO</sub>**)

Catalyst	Temperature (°C)	Time (minutes)	Activity (kg <sub>PE</sub> mol <sub>Zr</sub> <sup>-1</sup> h <sup>-1</sup> bar <sup>-1</sup> )	<i>M</i> <sub>w</sub> (kg mol <sup>-1</sup> )	<i>M</i> <sub>w</sub> / <i>M</i> <sub>n</sub>
<b>3<sub>sMAO</sub></b>	50	30	5056 ± 11	172	3.3
<b>3<sub>sMAO</sub></b>	60	30	4604 ± 89	126	3.2
<b>3<sub>sMAO</sub></b>	70	30	4233 ± 160	103	3.4
<b>3<sub>sMAO</sub></b>	80	30	3646 ± 282	67	3.3
<b>3<sub>sMAO</sub></b>	90	30	2686 ± 257	59	3.5
<b>3<sub>sMAO</sub></b>	80	5	6294 ± 239	-	-
<b>3<sub>sMAO</sub></b>	80	15	5353 ± 164	-	-
<b>3<sub>sMAO</sub></b>	80	60	3160 ± 222	-	-

Polymerisation conditions: [Al]<sub>0</sub>:[Zr]<sub>0</sub> = 200:1, 150 mg TiBA scavenger, 2 bar ethylene, 10 mg pre-catalyst, 50 mL hexane.

**Table S9.** Slurry-phase ethylene polymerisation with sMAO-<sup>Me<sub>2</sub></sup>SB(Cp,I\*)Zr(CH<sub>2</sub>Ph)<sub>2</sub> (**4<sub>s</sub>MAO**)

Catalyst	[Al] <sub>0</sub> /[Zr] <sub>0</sub>	Temperature (°C)	Time (minutes)	Activity (kg <sub>PE</sub> mol <sub>Zr</sub> <sup>-1</sup> h <sup>-1</sup> bar <sup>-1</sup> )	<i>M</i> <sub>w</sub> (kg mol <sup>-1</sup> )	<i>M</i> <sub>w</sub> / <i>M</i> <sub>n</sub>
<b>4<sub>s</sub>MAO</b>	300	50	30	7304 ± 237	-	-
<b>4<sub>s</sub>MAO</b>	300	60	30	6964 ± 209	-	-
<b>4<sub>s</sub>MAO</b>	300	70	30	6290 ± 48	-	-
<b>4<sub>s</sub>MAO</b>	300	80	30	5685 ± 267	-	-
<b>4<sub>s</sub>MAO</b>	300	90	30	4650 ± 107	-	-
<b>4<sub>s</sub>MAO</b>	200	50	30	6592 ± 59	216	2.8
<b>4<sub>s</sub>MAO</b>	200	60	30	6264 ± 143	130	3.0
<b>4<sub>s</sub>MAO</b>	200	70	30	6289 ± 225	102	3.1
<b>4<sub>s</sub>MAO</b>	200	80	30	5359 ± 49	84	2.8
<b>4<sub>s</sub>MAO</b>	200	90	30	3834 ± 80	81	3.0
<b>4<sub>s</sub>MAO</b>	200	80	5	9921 ± 943	-	-
<b>4<sub>s</sub>MAO</b>	200	80	15	6670 ± 31	-	-
<b>4<sub>s</sub>MAO</b>	200	80	60	4656 ± 15	-	-
<b>4<sub>s</sub>MAO</b>	100	50	30	3047 ± 140	-	-
<b>4<sub>s</sub>MAO</b>	100	60	30	2674 ± 63	-	-
<b>4<sub>s</sub>MAO</b>	100	70	30	2974 ± 91	-	-
<b>4<sub>s</sub>MAO</b>	100	80	30	2545 ± 36	-	-
<b>4<sub>s</sub>MAO</b>	100	90	30	2149 ± 58	-	-

Polymerisation conditions: 150 mg TiBA scavenger, 2 bar ethylene, 10 mg pre-catalyst, 50 mL hexane.

**Table S10.** Slurry-phase ethylene polymerisation with sMAO-<sup>Me<sub>2</sub></sup>SB(Cp<sup>Me</sup>,I\*)Zr(CH<sub>2</sub>Ph)<sub>2</sub> (**5<sub>s</sub>MAO**)

Catalyst	Temperature (°C)	Time (minutes)	Activity (kg <sub>PE</sub> mol <sub>Zr</sub> <sup>-1</sup> h <sup>-1</sup> bar <sup>-1</sup> )	<i>M</i> <sub>w</sub> (kg mol <sup>-1</sup> )	<i>M</i> <sub>w</sub> / <i>M</i> <sub>n</sub>
<b>5<sub>s</sub>MAO</b>	50	30	6353 ± 184	141	3.6
<b>5<sub>s</sub>MAO</b>	60	30	6729 ± 393	110	3.7
<b>5<sub>s</sub>MAO</b>	70	30	6504 ± 505	92	3.3
<b>5<sub>s</sub>MAO</b>	80	30	5566 ± 173	74	3.7
<b>5<sub>s</sub>MAO</b>	90	30	4559 ± 293	64	4.1
<b>5<sub>s</sub>MAO</b>	80	5	9509 ± 571	-	-
<b>5<sub>s</sub>MAO</b>	80	15	6644 ± 465	-	-
<b>5<sub>s</sub>MAO</b>	80	60	4424 ± 314	-	-

Polymerisation conditions: [Al]<sub>0</sub>:[Zr]<sub>0</sub> = 200:1, 150 mg TiBA scavenger, 2 bar ethylene, 10 mg pre-catalyst, 50 mL hexane.

**Table S11.** Slurry-phase ethylene polymerisation with sMAO-<sup>Me<sub>2</sub></sup>SB(Cp,I\*)ZrMe<sub>2</sub> (**6<sub>sMAO</sub>**)

Catalyst	[Al] <sub>0</sub> /[Zr] <sub>0</sub>	Temperature (°C)	Time (minutes)	Activity (kg <sub>PE</sub> mol <sub>Zr</sub> <sup>-1</sup> h <sup>-1</sup> bar <sup>-1</sup> )	<i>M</i> <sub>w</sub> (kg mol <sup>-1</sup> )	<i>M</i> <sub>w</sub> / <i>M</i> <sub>n</sub>
<b>6<sub>sMAO</sub></b>	300	50	30	7513 ± 277	-	-
<b>6<sub>sMAO</sub></b>	300	60	30	7492 ± 155	-	-
<b>6<sub>sMAO</sub></b>	300	70	30	6680 ± 215	-	-
<b>6<sub>sMAO</sub></b>	300	80	30	5856 ± 16	-	-
<b>6<sub>sMAO</sub></b>	300	90	30	4280 ± 264	-	-
<b>6<sub>sMAO</sub></b>	200	50	30	7533 ± 408	133	3.4
<b>6<sub>sMAO</sub></b>	200	60	30	7396 ± 131	96	3.4
<b>6<sub>sMAO</sub></b>	200	70	30	6551 ± 86	82	3.5
<b>6<sub>sMAO</sub></b>	200	80	30	5482 ± 135	61	3.4
<b>6<sub>sMAO</sub></b>	200	90	30	3935 ± 251	53	3.8
<b>6<sub>sMAO</sub></b>	200	80	5	8092 ± 360	-	-
<b>6<sub>sMAO</sub></b>	200	80	15	5520 ± 425	-	-
<b>6<sub>sMAO</sub></b>	200	80	60	3265 ± 128	-	-
<b>6<sub>sMAO</sub></b>	100	50	30	1798 ± 35	-	-
<b>6<sub>sMAO</sub></b>	100	60	30	2123 ± 104	-	-
<b>6<sub>sMAO</sub></b>	100	70	30	2126 ± 150	-	-
<b>6<sub>sMAO</sub></b>	100	80	30	2030 ± 24	-	-
<b>6<sub>sMAO</sub></b>	100	90	30	1619 ± 133	-	-

Polymerisation conditions: 150 mg TiBA scavenger, 2 bar ethylene, 10 mg pre-catalyst, 50 mL hexane.

**Table S12.** Slurry-phase ethylene polymerisation with sMAO- $\text{Me}_2\text{SB}(\text{Cp}^{\text{Me}}, \text{I}^*)\text{ZrMe}_2$  ( $\mathbf{7}_{\text{sMAO}}$ )

Catalyst	Temperature (°C)	Time (minutes)	Activity (kg <sub>PE</sub> mol <sub>Zr</sub> <sup>-1</sup> h <sup>-1</sup> bar <sup>-1</sup> )	$M_w$ (kg mol <sup>-1</sup> )	$M_w/M_n$
$\mathbf{7}_{\text{sMAO}}$	50	30	$7197 \pm 352$	112	4.2
$\mathbf{7}_{\text{sMAO}}$	60	30	$7948 \pm 44$	86	4.0
$\mathbf{7}_{\text{sMAO}}$	70	30	$6745 \pm 94$	72	4.2
$\mathbf{7}_{\text{sMAO}}$	80	30	$6346 \pm 170$	56	4.3
$\mathbf{7}_{\text{sMAO}}$	90	30	$4382 \pm 385$	48	4.0
$\mathbf{7}_{\text{sMAO}}$	80	5	$9509 \pm 571$	-	-
$\mathbf{7}_{\text{sMAO}}$	80	15	$6644 \pm 465$	-	-
$\mathbf{7}_{\text{sMAO}}$	80	60	$4424 \pm 314$	-	-

Polymerisation conditions:  $[\text{Al}]_0:[\text{Zr}]_0 = 200:1$ , 150 mg TiBA scavenger, 2 bar ethylene, 10 mg pre-catalyst, 50 mL hexane.

**Table S13.** Slurry-phase ethylene polymerisation with sMAO-(Cp<sup>nBu</sup>)<sub>2</sub>ZrCl<sub>2</sub>

Catalyst	Temperature (°C)	Time (minutes)	Activity (kg <sub>PE</sub> mol <sub>Zr</sub> <sup>-1</sup> h <sup>-1</sup> bar <sup>-1</sup> )	$M_w$ (kg mol <sup>-1</sup> )	$M_w/M_n$
$((\text{Cp}^{n\text{Bu}})_2\text{ZrCl}_2)_{\text{sMAO}}$	50	30	$4362 \pm 56$	222	2.9
$((\text{Cp}^{n\text{Bu}})_2\text{ZrCl}_2)_{\text{sMAO}}$	60	30	$4641 \pm 18$	201	2.8
$((\text{Cp}^{n\text{Bu}})_2\text{ZrCl}_2)_{\text{sMAO}}$	70	30	$4161 \pm 126$	159	3.2
$((\text{Cp}^{n\text{Bu}})_2\text{ZrCl}_2)_{\text{sMAO}}$	80	30	$3459 \pm 200$	130	3.3
$((\text{Cp}^{n\text{Bu}})_2\text{ZrCl}_2)_{\text{sMAO}}$	90	30	$2348 \pm 50$	93	3.1
$((\text{Cp}^{n\text{Bu}})_2\text{ZrCl}_2)_{\text{sMAO}}$	80	5	$7122 \pm 122$	-	-
$((\text{Cp}^{n\text{Bu}})_2\text{ZrCl}_2)_{\text{sMAO}}$	80	15	$4187 \pm 231$	-	-
$((\text{Cp}^{n\text{Bu}})_2\text{ZrCl}_2)_{\text{sMAO}}$	80	60	$2389 \pm 46$	-	-

Polymerisation conditions:  $[\text{Al}]_0:[\text{Zr}]_0 = 200:1$ , 150 mg TiBA scavenger, 2 bar ethylene, 10 mg pre-catalyst, 50 mL hexane.

**Table S14.** Larger scale slurry-phase ethylene polymerisation with sMAO-<sup>Me<sub>2</sub></sup>SB(Cp,I\*)ZrCl<sub>2</sub> (**A<sub>sMAO</sub>**), sMAO-<sup>Me<sub>2</sub></sup>SB(Cp,I\*)Zr(CH<sub>2</sub>Ph)<sub>2</sub> (**4<sub>sMAO</sub>**), sMAO-<sup>Me<sub>2</sub></sup>SB(Cp<sup>Me</sup>,I\*)Zr(CH<sub>2</sub>Ph)<sub>2</sub> (**5<sub>sMAO</sub>**), and sMAO-<sup>Me<sub>2</sub></sup>SB(Cp,I\*)ZrMe<sub>2</sub> (**6<sub>sMAO</sub>**).

Catalyst	Temperature (°C)	Time (minutes)	Activity (kg <sub>PE</sub> mol <sub>Zr</sub> <sup>-1</sup> h <sup>-1</sup> bar <sup>-1</sup> )	M <sub>w</sub> (kg mol <sup>-1</sup> )	M <sub>w</sub> /M <sub>n</sub>
<b>A<sub>sMAO</sub></b>	80	30	9160	142	4.1
<b>4<sub>sMAO</sub></b>	80	30	10773	168	3.6
<b>5<sub>sMAO</sub></b>	80	30	11898	156	3.9
<b>6<sub>sMAO</sub></b>	80	30	12036	136	3.0

Polymerisation conditions: [Al]<sub>0</sub>:[Zr]<sub>0</sub> = 200:1, 750 mg TiBA scavenger, 2 bar ethylene, 10 mg pre-catalyst, 250 mL hexane.

**Table S15.** Slurry-phase ethylene polymerisation with LDHMAO-<sup>Me<sub>2</sub></sup>SB(Cp,I\*)ZrCl<sub>2</sub> (**A<sub>LDHMAO</sub>**)

Catalyst	Temperature (°C)	Time (minutes)	Activity (kg <sub>PE</sub> mol <sub>Zr</sub> <sup>-1</sup> h <sup>-1</sup> bar <sup>-1</sup> )
<b>A<sub>LDHMAO</sub></b>	50	30	31 ± 1
<b>A<sub>LDHMAO</sub></b>	60	30	68 ± 2
<b>A<sub>LDHMAO</sub></b>	70	30	80 ± 11
<b>A<sub>LDHMAO</sub></b>	80	30	87 ± 6
<b>A<sub>LDHMAO</sub></b>	90	30	69 ± 9
<b>A<sub>LDHMAO</sub></b>	80	5	131 ± 8
<b>A<sub>LDHMAO</sub></b>	80	15	105 ± 9
<b>A<sub>LDHMAO</sub></b>	80	60	55 ± 7

Polymerisation conditions: [Al]<sub>0</sub>:[Zr]<sub>0</sub> = 200:1, 150 mg TiBA scavenger, 2 bar ethylene, 10 mg pre-catalyst, 50 mL hexane.

**Table S16.** Slurry-phase ethylene polymerisation with LDHMAO-<sup>Me2</sup>SB(Cp<sup>Me</sup>,I\*)ZrCl<sub>2</sub> (**B<sub>LDHMAO</sub>**)

Catalyst	Temperature (°C)	Time (minutes)	Activity (kg <sub>PE</sub> mol <sub>Zr</sub> <sup>-1</sup> h <sup>-1</sup> bar <sup>-1</sup> )
<b>B<sub>LDHMAO</sub></b>	50	30	235 ± 19
<b>B<sub>LDHMAO</sub></b>	60	30	310 ± 35
<b>B<sub>LDHMAO</sub></b>	70	30	254 ± 31
<b>B<sub>LDHMAO</sub></b>	80	30	214 ± 7
<b>B<sub>LDHMAO</sub></b>	90	30	274 ± 99
<b>B<sub>LDHMAO</sub></b>	80	5	433 ± 21
<b>B<sub>LDHMAO</sub></b>	80	15	307 ± 3
<b>B<sub>LDHMAO</sub></b>	80	60	185 ± 6

Polymerisation conditions: [Al]<sub>0</sub>:[Zr]<sub>0</sub> = 200:1, 150 mg TiBA scavenger, 2 bar ethylene, 10 mg pre-catalyst, 50 mL hexane.

**Table S17.** Slurry-phase ethylene polymerisation with LDHMAO-<sup>Me2</sup>SB(Cp,I\*)Zr(CH<sub>2</sub>Ph)<sub>2</sub> (**4<sub>LDHMAO</sub>**)

Catalyst	Temperature (°C)	Time (minutes)	Activity (kg <sub>PE</sub> mol <sub>Zr</sub> <sup>-1</sup> h <sup>-1</sup> bar <sup>-1</sup> )	M <sub>w</sub> (kg mol <sup>-1</sup> )	M <sub>w</sub> /M <sub>n</sub>
<b>4<sub>LDHMAO</sub></b>	50	30	2423 ± 60	603	2.9
<b>4<sub>LDHMAO</sub></b>	60	30	1513 ± 227	435	2.8
<b>4<sub>LDHMAO</sub></b>	70	30	1571 ± 203	423	2.8
<b>4<sub>LDHMAO</sub></b>	80	30	3182 ± 12	253	2.8
<b>4<sub>LDHMAO</sub></b>	90	30	1375 ± 254	228	2.7
<b>4<sub>LDHMAO</sub></b>	80	5	3787 ± 71	-	-
<b>4<sub>LDHMAO</sub></b>	80	15	3158 ± 39	-	-
<b>4<sub>LDHMAO</sub></b>	80	60	2227 ± 165	-	-

Polymerisation conditions: [Al]<sub>0</sub>:[Zr]<sub>0</sub> = 200:1, 150 mg TiBA scavenger, 2 bar ethylene, 10 mg pre-catalyst, 50 mL hexane.

**Table S18.** Slurry-phase ethylene polymerisation with LDHMAO-<sup>Me2</sup>SB(Cp,I\*)ZrMe<sub>2</sub> (**6<sub>LDHMAO</sub>**)

Catalyst	Temperature (°C)	Time (minutes)	Activity (kg <sub>PE</sub> mol <sub>Zr</sub> <sup>-1</sup> h <sup>-1</sup> bar <sup>-1</sup> )
<b>6<sub>LDHMAO</sub></b>	50	30	607 ± 6
<b>6<sub>LDHMAO</sub></b>	60	30	574 ± 26
<b>6<sub>LDHMAO</sub></b>	70	30	967 ± 35
<b>6<sub>LDHMAO</sub></b>	80	30	954 ± 19
<b>6<sub>LDHMAO</sub></b>	90	30	727 ± 2
<b>6<sub>LDHMAO</sub></b>	80	5	1388 ± 27
<b>6<sub>LDHMAO</sub></b>	80	15	1257 ± 82
<b>6<sub>LDHMAO</sub></b>	80	60	592 ± 23

Polymerisation conditions: [Al]<sub>0</sub>:[Zr]<sub>0</sub> = 200:1, 150 mg TiBA scavenger, 2 bar ethylene, 10 mg pre-catalyst, 50 mL hexane.

**Table S19.** Slurry-phase ethylene polymerisation with SSMAO-<sup>Me2</sup>SB(Cp,I\*)ZrCl<sub>2</sub> (**A<sub>SSMAO</sub>**)

Catalyst	Temperature (°C)	Time (minutes)	Activity (kg <sub>PE</sub> mol <sub>Zr</sub> <sup>-1</sup> h <sup>-1</sup> bar <sup>-1</sup> )	M <sub>w</sub> (kg mol <sup>-1</sup> )	M <sub>w</sub> /M <sub>n</sub>
<b>A<sub>SSMAO</sub></b>	50	30	659 ± 36	562	3.1
<b>A<sub>SSMAO</sub></b>	60	30	977 ± 41	408	2.8
<b>A<sub>SSMAO</sub></b>	70	30	959 ± 54	367	2.9
<b>A<sub>SSMAO</sub></b>	80	30	1192 ± 16	294	2.9
<b>A<sub>SSMAO</sub></b>	90	30	932 ± 65	242	3.1
<b>A<sub>SSMAO</sub></b>	80	5	788 ± 100	-	-
<b>A<sub>SSMAO</sub></b>	80	15	546 ± 27	-	-
<b>A<sub>SSMAO</sub></b>	80	60	415 ± 18	-	-

Polymerisation conditions: [Al]<sub>s</sub>:[Zr]<sub>0</sub> = 200:1, 150 mg TiBA scavenger, 2 bar ethylene, 10 mg pre-catalyst, 50 mL hexane.

**Table S20.** Slurry-phase ethylene polymerisation with SSMAO-<sup>Me2</sup>SB(Cp<sup>Me</sup>,I\*)ZrCl<sub>2</sub> (**B<sub>SSMAO</sub>**)

Catalyst	Temperature (°C)	Time (minutes)	Activity (kg <sub>PE</sub> mol <sub>Zr</sub> <sup>-1</sup> h <sup>-1</sup> bar <sup>-1</sup> )	M <sub>w</sub> (kg mol <sup>-1</sup> )	M <sub>w</sub> /M <sub>n</sub>
<b>B<sub>SSMAO</sub></b>	50	30	309 ± 11	518	3.2
<b>B<sub>SSMAO</sub></b>	60	30	445 ± 1	390	3.2
<b>B<sub>SSMAO</sub></b>	70	30	490 ± 8	343	3.1
<b>B<sub>SSMAO</sub></b>	80	30	666 ± 1	270	3.2
<b>B<sub>SSMAO</sub></b>	90	30	564 ± 38	241	3.3
<b>B<sub>SSMAO</sub></b>	80	5	854 ± 2	-	-
<b>B<sub>SSMAO</sub></b>	80	15	706 ± 2	-	-
<b>B<sub>SSMAO</sub></b>	80	60	550 ± 18	-	-

Polymerisation conditions: [Al]<sub>0</sub>:[Zr]<sub>0</sub> = 200:1, 150 mg TiBA scavenger, 2 bar ethylene, 10 mg pre-catalyst, 50 mL hexane.

**Table S21.** Slurry-phase ethylene polymerisation with SSMAO-<sup>Me2</sup>SB(Cp,I\*)Zr(CH<sub>2</sub>Ph)<sub>2</sub> (**4<sub>SSMAO</sub>**)

Catalyst	Temperature (°C)	Time (minutes)	Activity (kg <sub>PE</sub> mol <sub>Zr</sub> <sup>-1</sup> h <sup>-1</sup> bar <sup>-1</sup> )	M <sub>w</sub> (kg mol <sup>-1</sup> )	M <sub>w</sub> /M <sub>n</sub>
<b>4<sub>SSMAO</sub></b>	50	30	610 ± 68	699	3.1
<b>4<sub>SSMAO</sub></b>	60	30	913 ± 38	520	3.0
<b>4<sub>SSMAO</sub></b>	70	30	991 ± 16	429	2.9
<b>4<sub>SSMAO</sub></b>	80	30	1168 ± 27	316	2.9
<b>4<sub>SSMAO</sub></b>	90	30	1121 ± 6	251	3.0
<b>4<sub>SSMAO</sub></b>	80	5	1364 ± 36	-	-
<b>4<sub>SSMAO</sub></b>	80	15	1159 ± 28	-	-
<b>4<sub>SSMAO</sub></b>	80	60	1040 ± 41	-	-

Polymerisation conditions: [Al]<sub>0</sub>:[Zr]<sub>0</sub> = 200:1, 150 mg TiBA scavenger, 2 bar ethylene, 10 mg pre-catalyst, 50 mL hexane.

**Table S22.** Slurry-phase ethylene polymerisation with SSMAO-<sup>Me<sub>2</sub></sup>SB(Cp,I\*)ZrMe<sub>2</sub> (**6<sub>SSMAO</sub>**)

Catalyst	Temperature (°C)	Time (minutes)	Activity (kg <sub>PE</sub> mol <sub>Zr</sub> <sup>-1</sup> h <sup>-1</sup> bar <sup>-1</sup> )	<i>M</i> <sub>w</sub> (kg mol <sup>-1</sup> )	<i>M</i> <sub>w</sub> / <i>M</i> <sub>n</sub>
<b>6<sub>SSMAO</sub></b>	50	30	683 ± 9	689	3.0
<b>6<sub>SSMAO</sub></b>	60	30	775 ± 21	503	3.0
<b>6<sub>SSMAO</sub></b>	70	30	1125 ± 23	399	2.9
<b>6<sub>SSMAO</sub></b>	80	30	1227 ± 46	325	2.8
<b>6<sub>SSMAO</sub></b>	90	30	1119 ± 33	232	2.9
<b>6<sub>SSMAO</sub></b>	80	5	1519 ± 13	-	-
<b>6<sub>SSMAO</sub></b>	80	15	1312 ± 53	-	-
<b>6<sub>SSMAO</sub></b>	80	60	986 ± 47	-	-

Polymerisation conditions: [Al]<sub>0</sub>:[Zr]<sub>0</sub> = 200:1, 150 mg TiBA scavenger, 2 bar ethylene, 10 mg pre-catalyst, 50 mL hexane.

**Table S23.** Crystallisation temperature ( $T_c$ ), enthalpy of crystallisation ( $\Delta H_c$ ) melting temperature ( $T_m$ ) and enthalpy of melting ( $\Delta H_m$ ) of the polyethylene produced from **A<sub>s</sub>MAO**, **B<sub>s</sub>MAO**, **1<sub>s</sub>MAO**, **2<sub>s</sub>MAO**, **3<sub>s</sub>MAO**, **4<sub>s</sub>MAO**, **5<sub>s</sub>MAO**, **6<sub>s</sub>MAO** and **7<sub>s</sub>MAO**.

Catalyst	$T_c$ (°C)	$\Delta H_c$ (J g <sup>-1</sup> )	$T_m$ (°C)	$\Delta H_m$ (J g <sup>-1</sup> )	% crystallinity
<b>A<sub>s</sub>MAO</b>	122	208	133	220	75
<b>B<sub>s</sub>MAO</b>	121	208	133	212	72
<b>E-1<sub>s</sub>MAO</b>	121	206	132	196	67
<b>Z-1<sub>s</sub>MAO</b>	121	195	133	202	69
<b>2<sub>s</sub>MAO</b>	120	176	132	186	63
<b>3<sub>s</sub>MAO</b>	118	174	134	184	63
<b>4<sub>s</sub>MAO</b>	120	191	133	197	67
<b>5<sub>s</sub>MAO</b>	119	195	132	196	67
<b>6<sub>s</sub>MAO</b>	123	193	133	196	67
<b>7<sub>s</sub>MAO</b>	119	212	131	211	72

Polymerisation conditions:  $[Al]_0:[Zr]_0 = 200:1$ , 150 mg TiBA scavenger, 2 bar ethylene, 10 mg pre-catalyst, 50 mL hexane, 80 °C. % crystallinity =  $\frac{\Delta H_m}{\Delta H_m^\circ} \times 100\%$  where  $\Delta H_m^\circ$  = enthalpy of melting for 100% crystalline polyethylene (293 J g<sup>-1</sup>)

## 4.2 Additional polymerisation graphs

### Exemplar molecular weight distribution

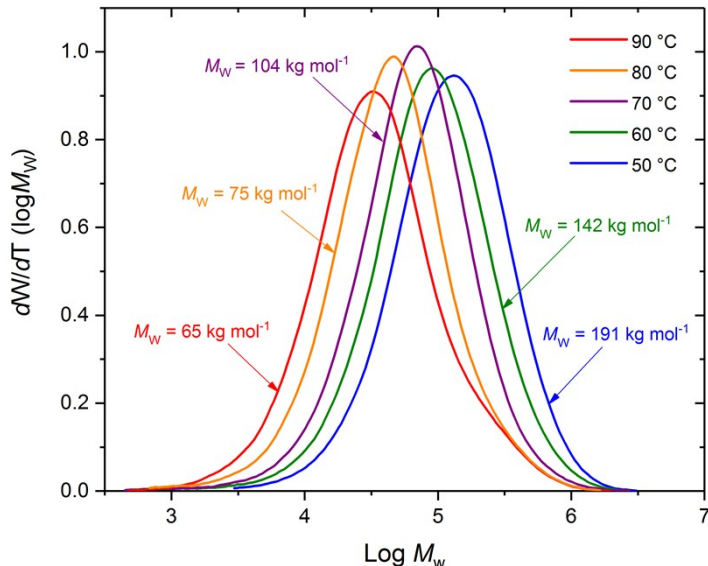


**Fig. S28.** Molecular weights distribution for  ${}^{\text{Me}_2}\text{SB}(\text{Cp},\text{I}^*)\text{ZrCl}_2$  ( $\mathbf{1}_{\text{sMAO}}$ ) at 50 °C (blue), 60 °C (green), 70 °C (purple), 80 °C (orange) and 90 °C (red), with molecular weights ( $M_w$ , kg mol<sup>-1</sup>) also given. Polymerisation conditions:  $[\text{Al}]_0:[\text{Zr}]_0 = 200:1$ , 150 mg TiBA scavenger, 2 bar ethylene, 10 mg pre-catalyst, 50 mL hexane, 30 minutes.

### Exemplar plot of polymerisation activity in function of time of polymerisation

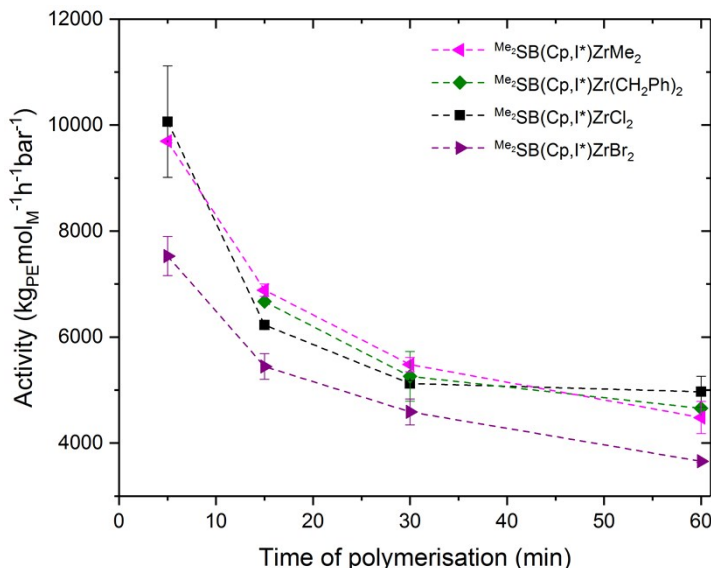


**Fig. S29.** Slurry-phase ethylene polymerisation activity in function of time of polymerisation for sMAO- ${}^{\text{Me}_2}\text{SB}(\text{Cp},\text{I}^*)\text{ZrMe}_2$  ( $\mathbf{6}_{\text{sMAO}}$ ) (pink left triangle), sMAO- ${}^{\text{Me}_2}\text{SB}(\text{Cp},\text{I}^*)\text{Zr}(\text{CH}_2\text{Ph})_2$  ( $\mathbf{4}_{\text{sMAO}}$ ) (green diamond), sMAO- ${}^{\text{Me}_2}\text{SB}(\text{Cp},\text{I}^*)\text{ZrCl}_2$  ( $\mathbf{A}_{\text{sMAO}}$ ) (black square) and sMAO- ${}^{\text{Me}_2}\text{SB}(\text{Cp},\text{I}^*)\text{ZrBr}_2$  ( $\mathbf{2}_{\text{sMAO}}$ ) (purple right triangle). Polymerisation conditions:

$[Al]_0:[Zr]_0 = 200:1$ , 150 mg TiBA scavenger, 2 bar ethylene, 10 mg pre-catalyst, 50 mL hexane, 80 °C.

### Exemplar plot of activity and molecular weights in function of time of polymerisation

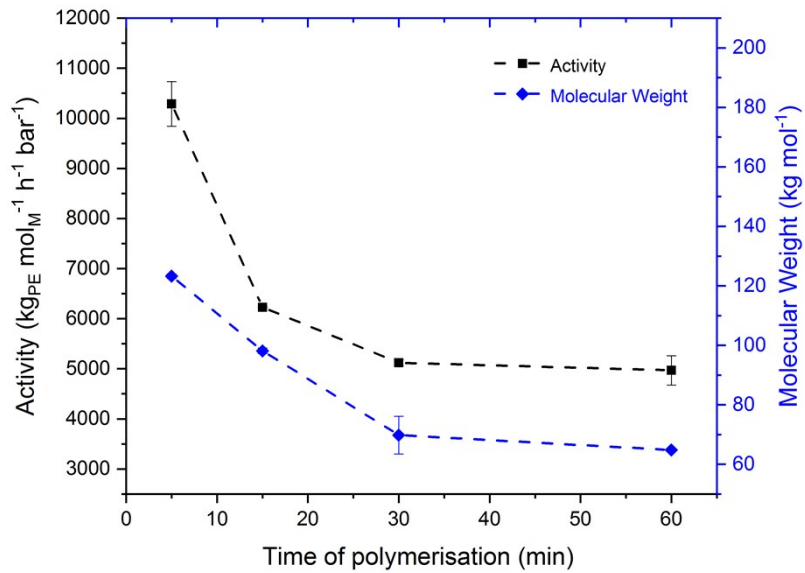


**Fig. S30.** Slurry-phase ethylene polymerisation activity (black square) and molecular weights ( $M_w$ ) (blue diamond) in function of time of polymerisation for sMAO- $\text{Me}_2\text{SB}(\text{Cp},\text{I}^*)\text{ZrCl}_2$  ( $\mathbf{A}_{\text{sMAO}}$ ). Polymerisation conditions:  $[Al]_0:[Zr]_0 = 200:1$ , 150 mg TiBA scavenger, 2 bar ethylene, 10 mg pre-catalyst, 50 mL hexane, 80 °C.

### Differential Scanning Calorimetry plots

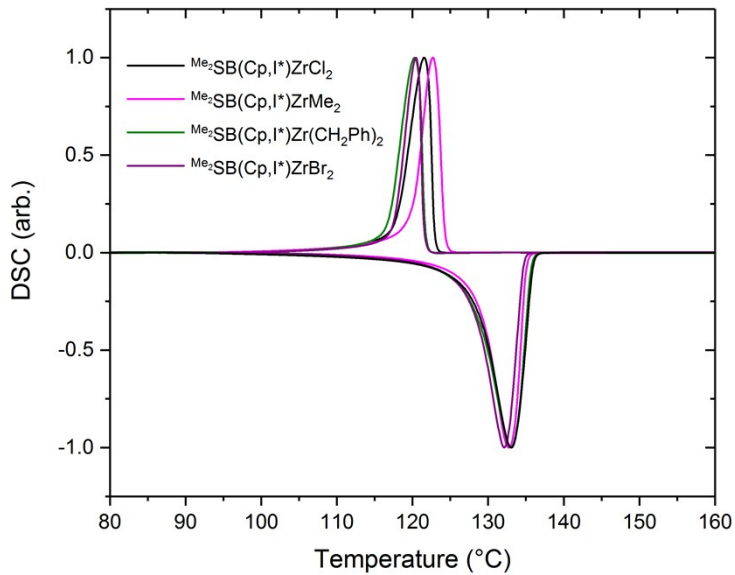


**Fig. S31.** Differential scanning calorimetry plot for the polyethylenes produced from sMAO- $\text{Me}_2\text{SB}(\text{Cp},\text{I}^*)\text{ZrCl}_2$  ( $\mathbf{A}_{\text{sMAO}}$ ) (black), sMAO- $\text{Me}_2\text{SB}(\text{Cp},\text{I}^*)\text{ZrBr}_2$  ( $\mathbf{2}_{\text{sMAO}}$ ) (purple), sMAO- $\text{Me}_2\text{SB}(\text{Cp},\text{I}^*)\text{Zr}(\text{CH}_2\text{Ph})_2$  ( $\mathbf{4}_{\text{sMAO}}$ ) (green) and sMAO- $\text{Me}_2\text{SB}(\text{Cp},\text{I}^*)\text{ZrMe}_2$  ( $\mathbf{6}_{\text{sMAO}}$ ) (pink). Polymerisation conditions:  $[Al]_0:[Zr]_0 = 200:1$ , 150 mg TiBA scavenger, 2 bar

ethylene, 10 mg pre-catalyst, 50 mL hexane, 30 minutes, 80 °C. Baseline and peak height normalised for clarity.

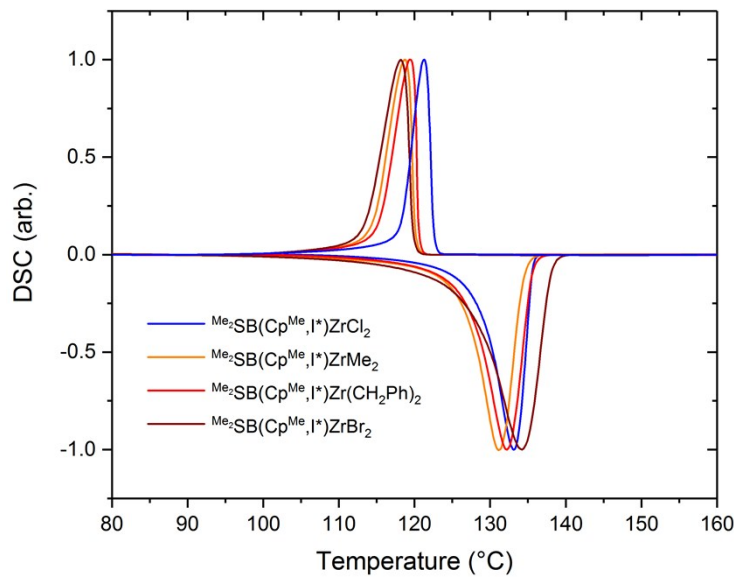


**Fig. S32.** Differential scanning calorimetry plot for the polyethylenes produced from sMAO- $\text{Me}_2\text{SB}(\text{Cp}^{\text{Me}}, \text{I}^*)\text{ZrCl}_2$  (**B<sub>sMAO</sub>**) (blue), sMAO- $\text{Me}_2\text{SB}(\text{Cp}^{\text{Me}}, \text{I}^*)\text{ZrBr}_2$  (**3<sub>sMAO</sub>**) (brown), sMAO- $\text{Me}_2\text{SB}(\text{Cp}^{\text{Me}}, \text{I}^*)\text{Zr}(\text{CH}_2\text{Ph})_2$  (**5<sub>sMAO</sub>**) (red) and sMAO- $\text{Me}_2\text{SB}(\text{Cp}^{\text{Me}}, \text{I}^*)\text{ZrMe}_2$  (**7<sub>sMAO</sub>**) (orange). Polymerisation conditions:  $[\text{Al}_{\text{sMAO}}]_0:[\text{Zr}]_0 = 200:1$ , 150 mg TiBA scavenger, 2 bar ethylene, 10 mg pre-catalyst, 50 mL hexane, 30 minutes, 80 °C. Baseline and peak height normalised for clarity.

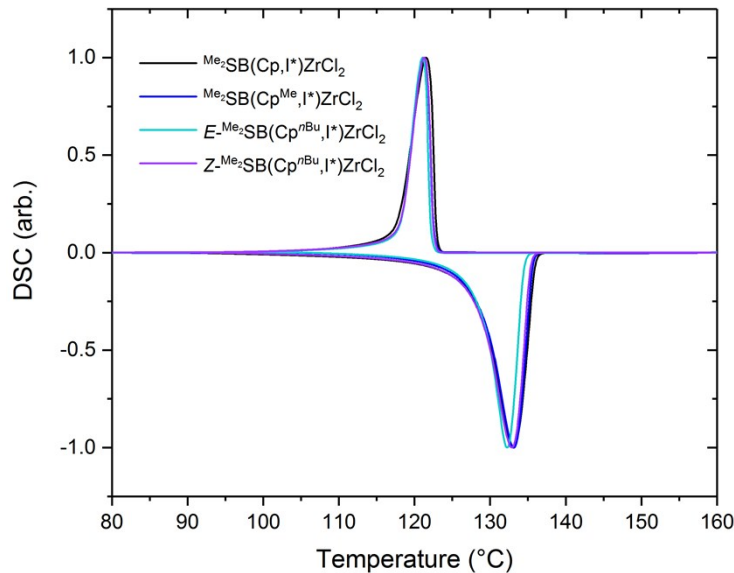


**Fig. S33.** Differential scanning calorimetry plot for the polyethylenes produced from sMAO- $\text{Me}_2\text{SB}(\text{Cp}, \text{I}^*)\text{ZrCl}_2$  (**A<sub>sMAO</sub>**) (black), sMAO- $\text{Me}_2\text{SB}(\text{Cp}^{\text{Me}}, \text{I}^*)\text{ZrBr}_2$  (**B<sub>sMAO</sub>**) (blue), sMAO- $E\text{-Me}_2\text{SB}(\text{Cp}^{n\text{Bu}}, \text{I}^*)\text{ZrCl}_2$  (**E-1<sub>sMAO</sub>**) (teal) and sMAO- $E\text{-Me}_2\text{SB}(\text{Cp}^{n\text{Bu}}, \text{I}^*)\text{ZrCl}_2$  (**Z-1<sub>sMAO</sub>**) (violet). Polymerisation conditions:  $[\text{Al}]_0:[\text{Zr}]_0 = 200:1$ , 150 mg TiBA scavenger,

2 bar ethylene, 10 mg pre-catalyst, 50 mL hexane, 30 minutes, 80 °C. Baseline and peak height normalised for clarity.

#### Exemplar plot of activity in function of amount of TiBA

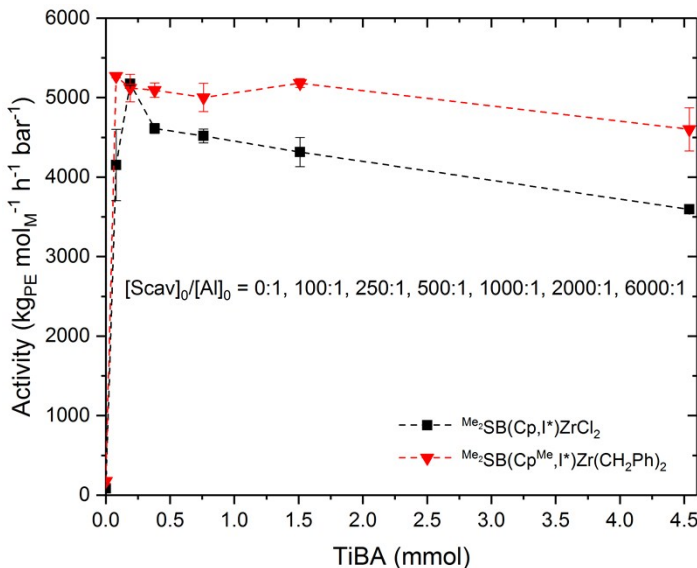


**Fig. S34.** Slurry-phase ethylene polymerisation activity in function of amount of TiBA scavenger (mmol) for sMAO- $\text{Me}_2\text{SB}(\text{Cp},\text{I}^*)\text{ZrCl}_2$  ( $\mathbf{A}_{\text{sMAO}}$ ) (black square), sMAO- $\text{Me}_2\text{SB}(\text{Cp}^{\text{Me}},\text{I}^*)\text{Zr}(\text{CH}_2\text{Ph})_2$  ( $\mathbf{5}_{\text{sMAO}}$ ) (red down triangle). Polymerisation conditions:  $[\text{Al}]_0:[\text{Zr}]_0 = 200:1$ , 2 bar ethylene, 10 mg pre-catalyst, 50 mL hexane, 80 °C.

#### Activity dependence in function of amount of zirconium

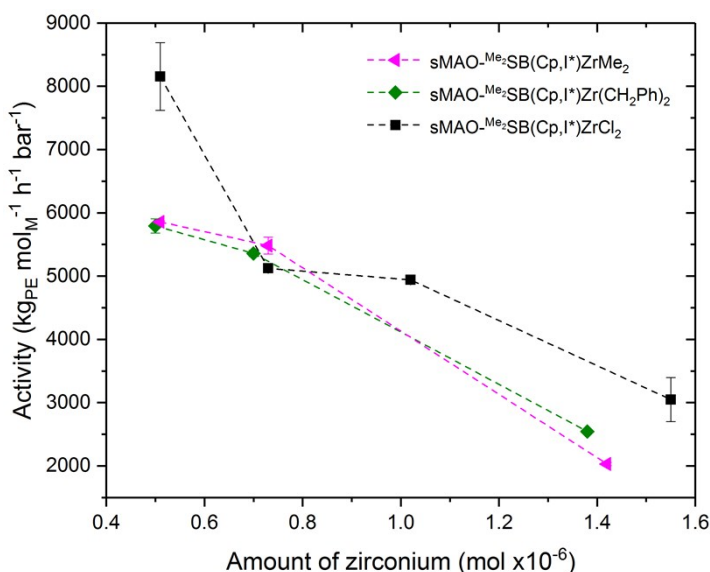


**Fig. S35.** Slurry-phase ethylene polymerisation activity in function of amount of zirconium for sMAO- $\text{Me}_2\text{SB}(\text{Cp},\text{I}^*)\text{ZrCl}_2$  ( $\mathbf{A}_{\text{sMAO}}$ ) (black square), sMAO- $\text{Me}_2\text{SB}(\text{Cp},\text{I}^*)\text{Zr}(\text{CH}_2\text{Ph})_2$  ( $\mathbf{4}_{\text{sMAO}}$ ) (green diamond) and sMAO- $\text{Me}_2\text{SB}(\text{Cp},\text{I}^*)\text{ZrMe}_2$  ( $\mathbf{6}_{\text{sMAO}}$ ) (pink left triangle).

Polymerisation conditions: 150 mg TiBA scavenger, 2 bar ethylene, 10 mg pre-catalyst, 50 mL hexane, 30 minutes, 80 °C.

#### Activity in function of temperature for $^{Me_2}SB(Cp,I^*)ZrCl_2$ (A) supported on sMAO, SSMAO and LDHMAO ( $A_{sMAO}$ , $A_{SSMAO}$ , $A_{LDHMAO}$ )

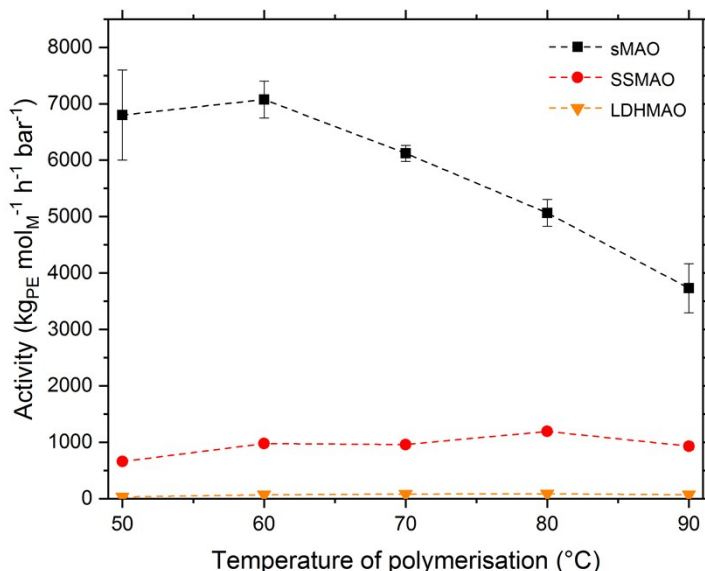


**Fig. S36.** Slurry-phase ethylene polymerisation activity in function of temperature of polymerisation for  $^{Me_2}SB(Cp,I^*)ZrCl_2$  supported on sMAO ( $A_{sMAO}$ ) (black square), LDHMAO ( $A_{LDHMAO}$ ) (orange down triangle) and SSMAO ( $A_{SSMAO}$ ) (red circle). Polymerisation conditions:  $[Al]_0:[Zr]_0 = 200:1$ , 150 mg TiBA scavenger, 2 bar ethylene, 10 mg pre-catalyst, 50 mL hexane, 30 minutes.

#### Activity in function of temperature for $^{Me_2}SB(Cp^{Me},I^*)ZrCl_2$ (B) supported on sMAO, SSMAO and LDHMAO ( $B_{sMAO}$ , $B_{SSMAO}$ , $B_{LDHMAO}$ )

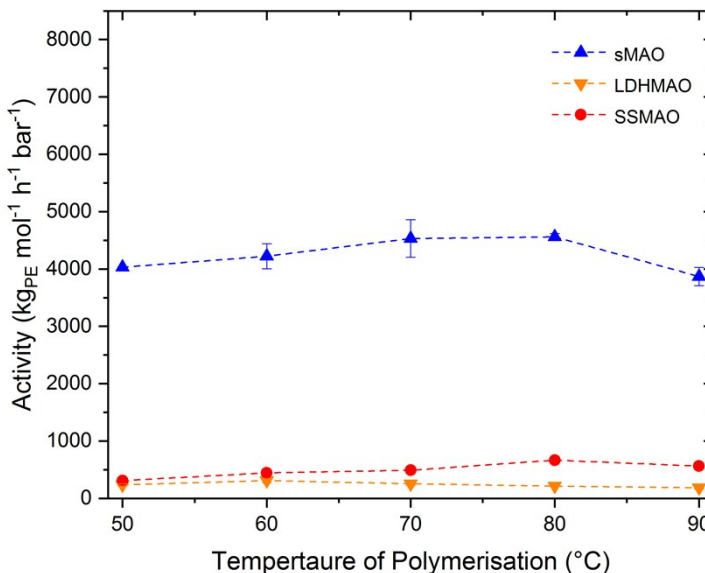


**Fig. S37.** Slurry-phase ethylene polymerisation activity in function of temperature of polymerisation for  $^{Me_2}SB(Cp^{Me},I^*)ZrCl_2$  supported on sMAO ( $B_{sMAO}$ ) (blue triangle),

LDHMAO (**B<sub>LDHMAO</sub>**) (orange down triangle) and SSMAO (**B<sub>SSMAO</sub>**) (red circle). Polymerisation conditions:  $[Al]_0:[Zr]_0 = 200:1$ , 150 mg TiBA scavenger, 2 bar ethylene, 10 mg pre-catalyst, 50 mL hexane, 30 minutes.

**Activity in function of temperature for  $^{Me_2}SB(Cp,I^*)ZrMe_2$  (6) supported on sMAO, SSMAO and LDHMAO ( $6_{sMAO}$ ,  $6_{SSMAO}$ ,  $6_{LDHMAO}$ )**

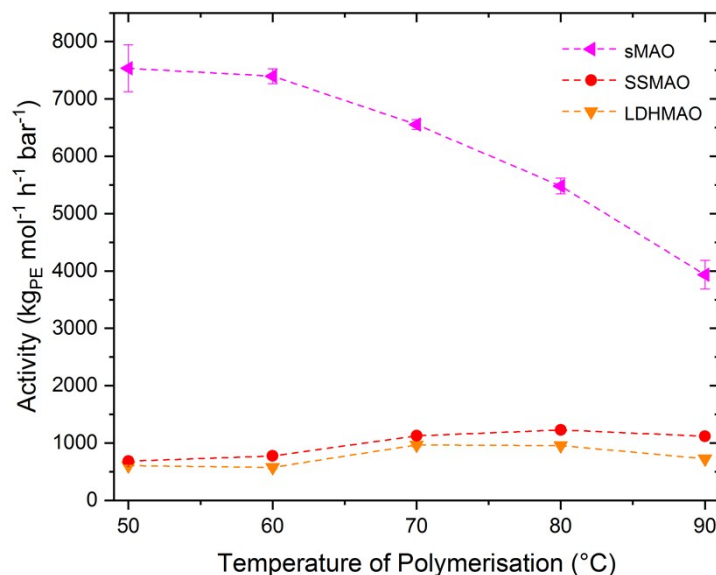


**Fig. S38.** Slurry-phase ethylene polymerisation activity in function of temperature of polymerisation for  $^{Me_2}SB(Cp,I^*)Zr(CH_2Ph)_2$  supported on sMAO ( $6_{sMAO}$ ) (pink left triangle), LDHMAO ( $6_{LDHMAO}$ ) (orange down triangle) and SSMAO ( $6_{SSMAO}$ ) (red circle). Polymerisation conditions:  $[Al]_0:[Zr]_0 = 200:1$ , 150 mg TiBA scavenger, 2 bar ethylene, 10 mg pre-catalyst, 50 mL hexane, 30 minutes.

#### 4.3 SEM Images

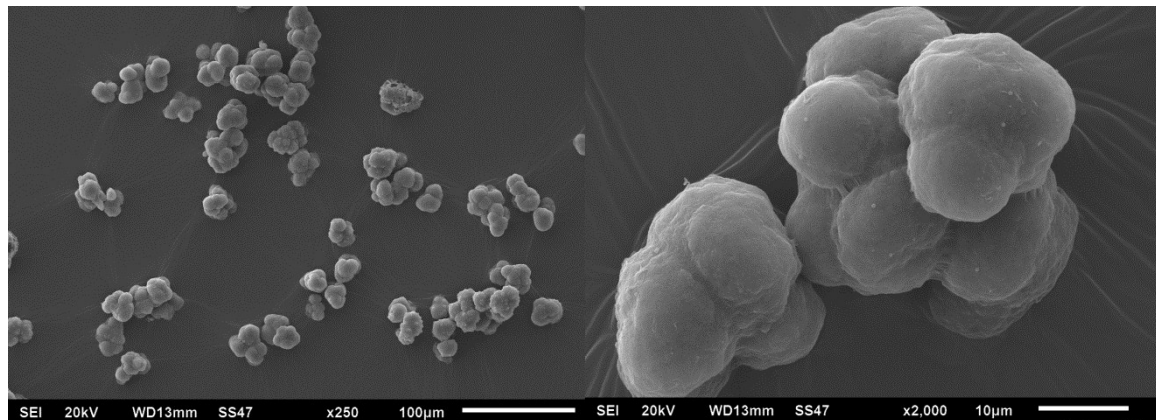


**Fig. S39.** SEM images of the polyethylenes synthesised using sMAO- $\text{Me}_2\text{SB}(\text{Cp},\text{I}^*)\text{ZrCl}_2$  (**A<sub>s</sub>MAO**). Polymerisation conditions:  $[\text{Al}]_0:[\text{Zr}]_0 = 200:1$ , 2 bar ethylene, 50 mL hexane, 10 mg pre-catalyst, 150 mg TIBA, 30 minutes.

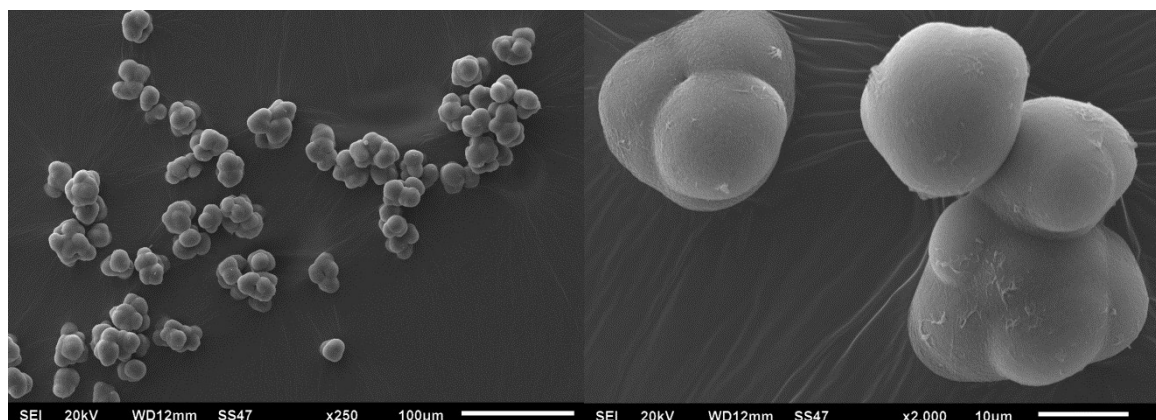


**Fig. S40.** SEM images of the polyethylenes synthesised using sMAO- $\text{Me}_2\text{SB}(\text{Cp}^{\text{Me}},\text{I}^*)\text{ZrCl}_2$  (**B<sub>s</sub>MAO**). Polymerisation conditions:  $[\text{Al}]_0:[\text{Zr}]_0 = 200:1$ , 2 bar ethylene, 50 mL hexane, 10 mg pre-catalyst, 150 mg TIBA, 30 minutes.

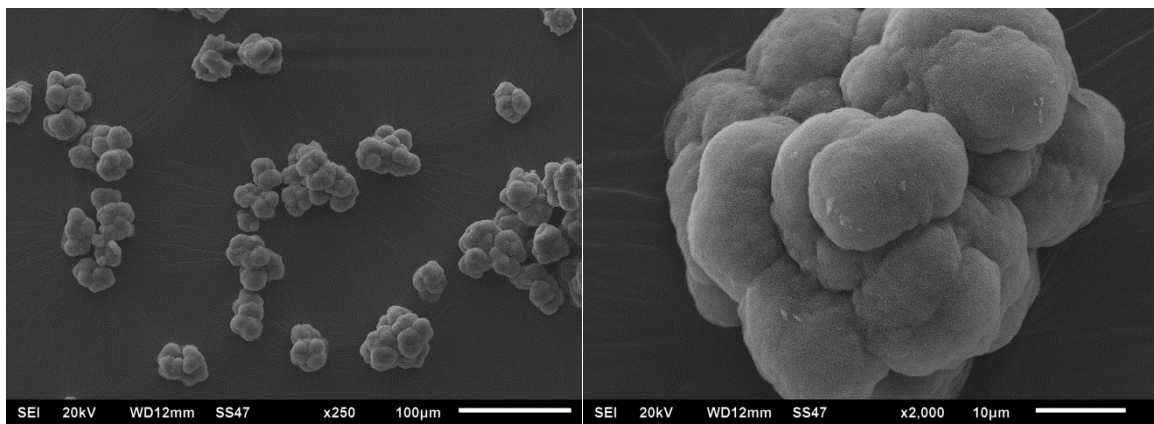


**Fig. S41.** SEM images of the polyethylenes synthesised using sMAO- $E\text{-Me}_2\text{SB}(\text{Cp}^n\text{Bu},\text{I}^*)\text{ZrCl}_2$  ( $\text{E-1}_{\text{sMAO}}$ ). Polymerisation conditions:  $[\text{Al}]_0:[\text{Zr}]_0 = 200:1$ , 2 bar ethylene, 50 mL hexane, 10 mg pre-catalyst, 150 mg TIBA, 30 minutes.

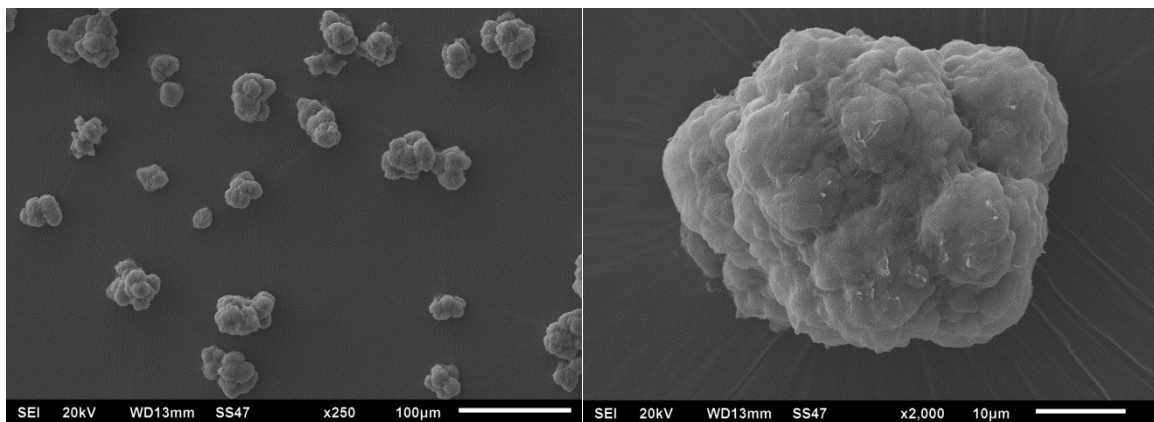


**Fig. S42.** SEM images of the polyethylenes synthesised using sMAO- $Z\text{-Me}_2\text{SB}(\text{Cp}^n\text{Bu},\text{I}^*)\text{ZrCl}_2$  ( $\text{Z-1}_{\text{sMAO}}$ ). Polymerisation conditions:  $[\text{Al}]_0:[\text{Zr}]_0 = 200:1$ , 2 bar ethylene, 50 mL hexane, 10 mg pre-catalyst, 150 mg TIBA, 30 minutes.

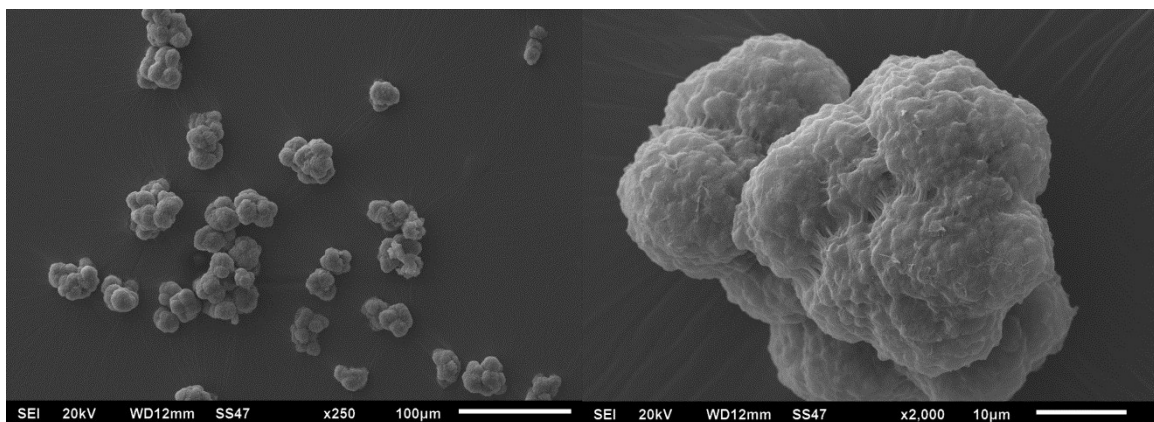


**Fig. S43.** SEM images of the polyethylenes synthesised using sMAO- $\text{-Me}_2\text{SB}(\text{Cp},\text{I}^*)\text{ZrBr}_2$  ( $\text{2}_{\text{sMAO}}$ ). Polymerisation conditions:  $[\text{Al}]_0:[\text{Zr}]_0 = 200:1$ , 2 bar ethylene, 50 mL hexane, 10 mg pre-catalyst, 150 mg TIBA, 30 minutes.

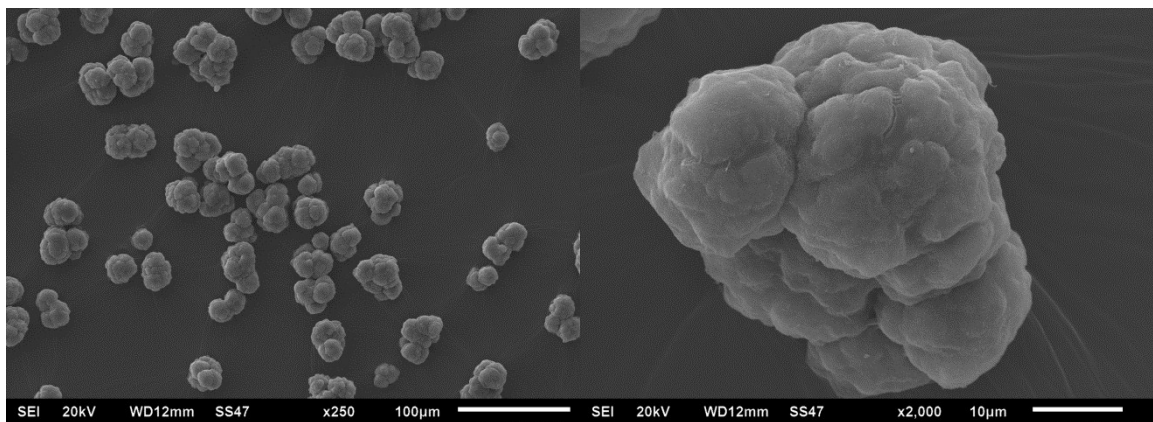


**Fig. S44.** SEM images of the polyethylenes synthesised using sMAO- $\text{Me}_2\text{SB}(\text{Cp}^{\text{Me}}, \text{I}^*)\text{ZrBr}_2$  ( $\mathbf{3}_{\text{sMAO}}$ ). Polymerisation conditions:  $[\text{Al}]_0:[\text{Zr}]_0 = 200:1$ , 2 bar ethylene, 50 mL hexane, 10 mg pre-catalyst, 150 mg TIBA, 30 minutes.

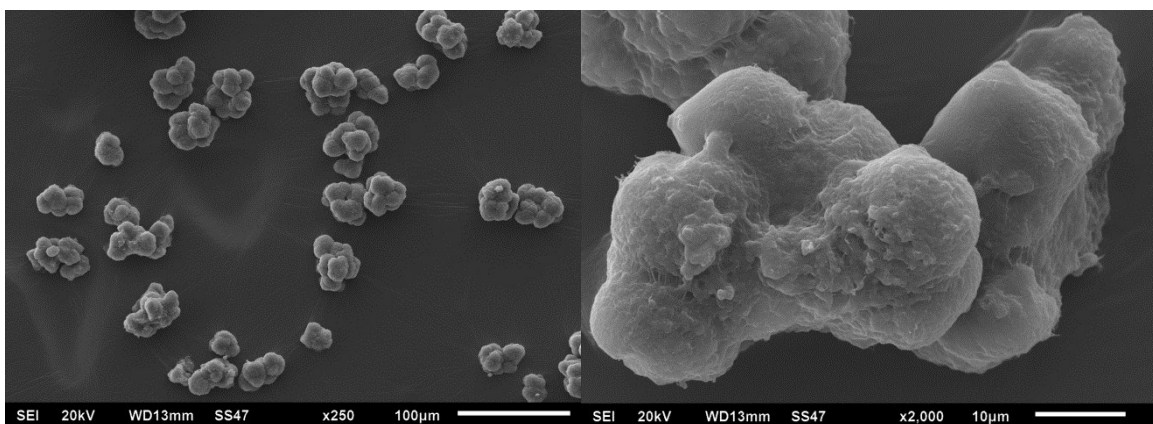


**Fig. S45.** SEM images of the polyethylenes synthesised using sMAO- $\text{Me}_2\text{SB}(\text{Cp}, \text{I}^*)\text{Zr}(\text{CH}_2\text{Ph})_2$  ( $\mathbf{4}_{\text{sMAO}}$ ). Polymerisation conditions:  $[\text{Al}]_0:[\text{Zr}]_0 = 200:1$ , 2 bar ethylene, 50 mL hexane, 10 mg pre-catalyst, 150 mg TIBA, 30 minutes.

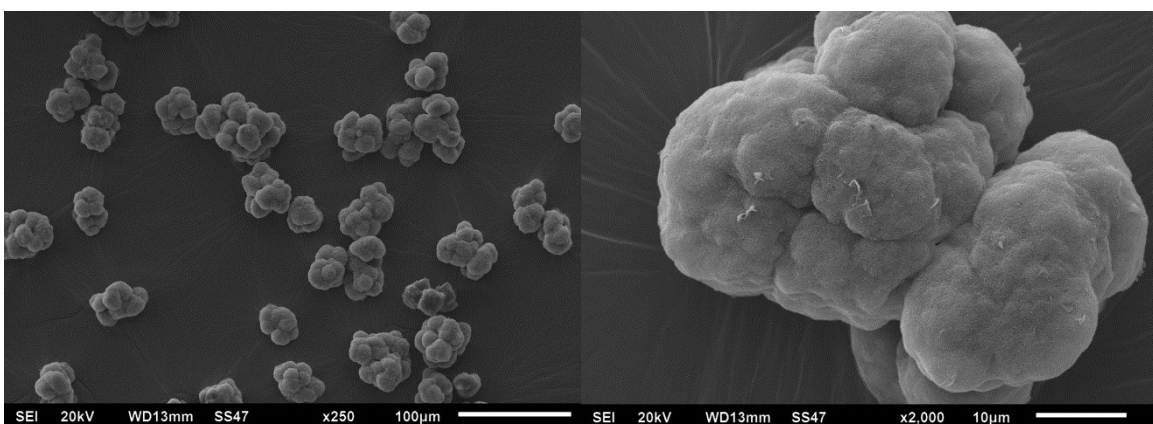


**Fig. S46.** SEM images of the polyethylenes synthesised using sMAO- $\text{Me}_2\text{SB}(\text{Cp}^{\text{Me}}, \text{I}^*)\text{Zr}(\text{CH}_2\text{Ph})_2$  ( $\mathbf{5}_{\text{sMAO}}$ ). Polymerisation conditions:  $[\text{Al}]_0:[\text{Zr}]_0 = 200:1$ , 2 bar ethylene, 50 mL hexane, 10 mg pre-catalyst, 150 mg TIBA, 30 minutes.

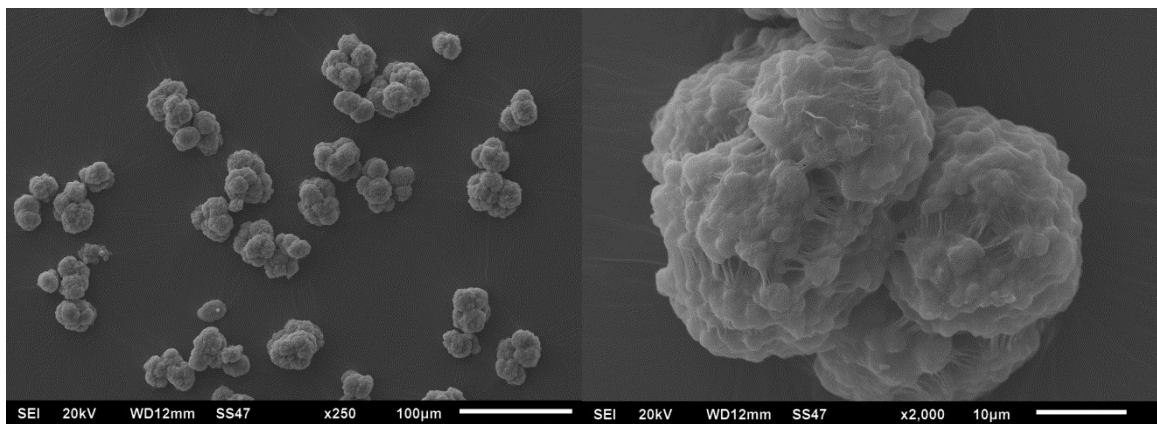


**Fig. S47.** SEM images of the polyethylenes synthesised using sMAO- $\text{Me}_2\text{SB}(\text{Cp},\text{I}^*)\text{ZrMe}_2$  (**6<sub>sMAO</sub>**). Polymerisation conditions:  $[\text{Al}]_0:[\text{Zr}]_0 = 200:1$ , 2 bar ethylene, 50 mL hexane, 10 mg pre-catalyst, 150 mg TIBA, 30 minutes.

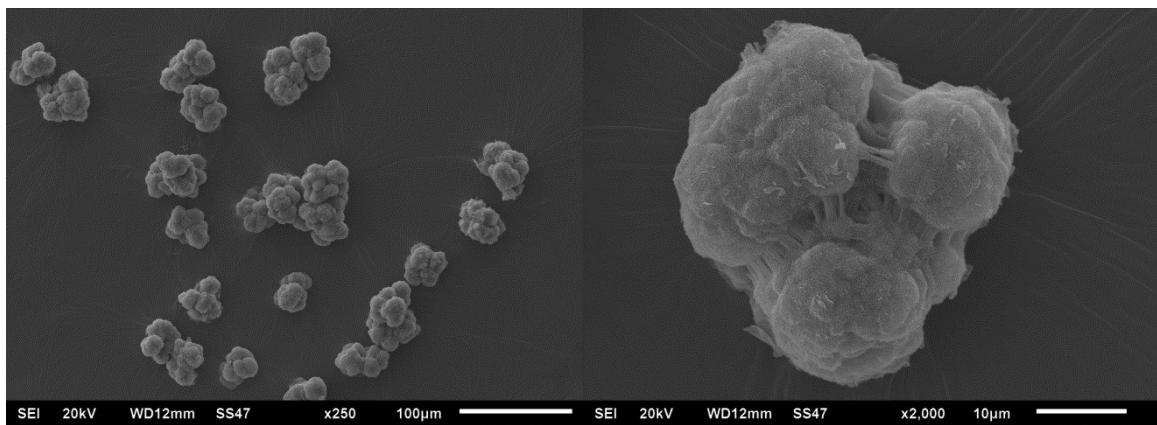


**Fig. S48.** SEM images of the polyethylenes synthesised using sMAO- $\text{Me}_2\text{SB}(\text{Cp}^{\text{Me}},\text{I}^*)\text{ZrMe}_2$  (**7<sub>sMAO</sub>**). Polymerisation conditions:  $[\text{Al}]_0:[\text{Zr}]_0 = 200:1$ , 2 bar ethylene, 50 mL hexane, 10 mg pre-catalyst, 150 mg TIBA, 30 minutes.

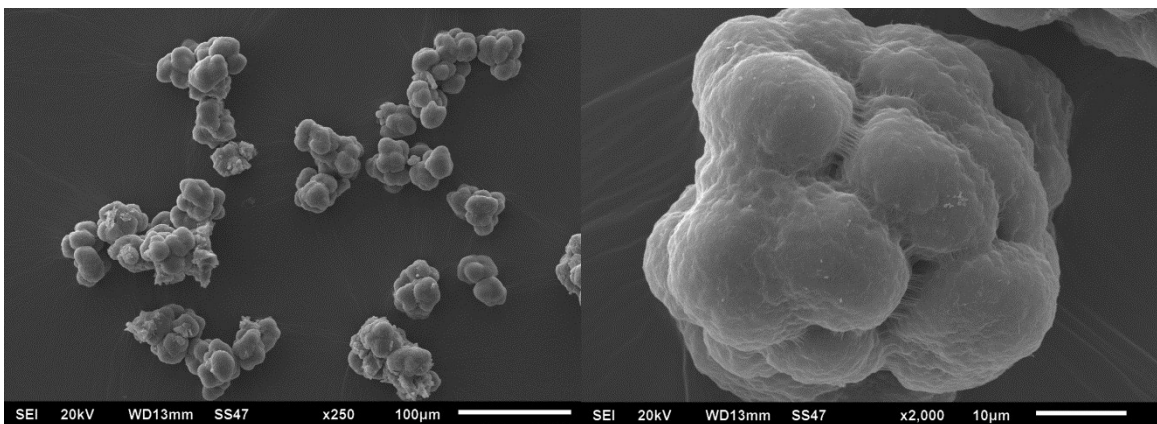


**Fig. S49.** SEM images of the polyethylenes synthesised using sMAO- $\text{Me}_2\text{SB}(\text{Cp},\text{I}^*)\text{ZrCl}_2$  (**A<sub>sMAO</sub>**) on the larger scale. Polymerisation conditions:  $[\text{Al}]_0:[\text{Zr}]_0 = 200:1$ , 2 bar ethylene, 250 mL hexane, 10 mg pre-catalyst, 750 mg TIBA, 30 minutes.

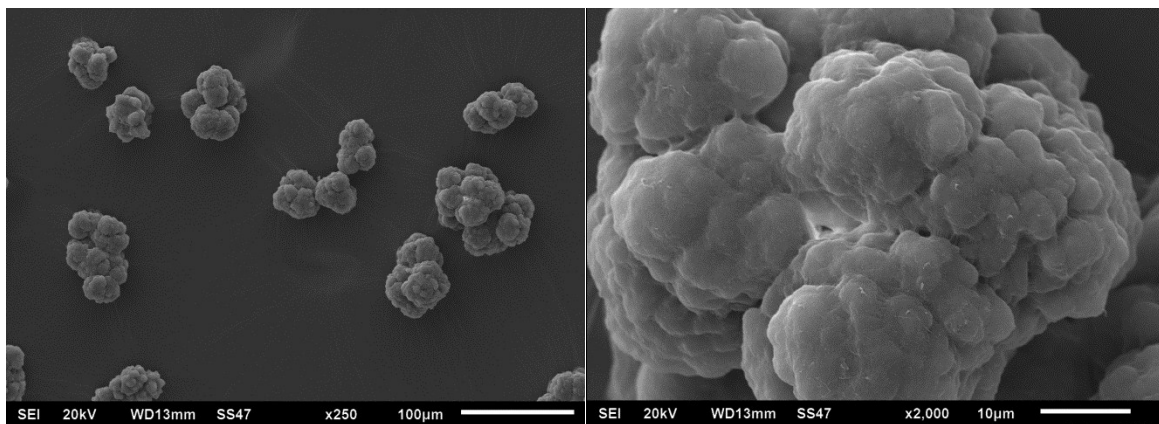


**Fig. S50.** SEM images of the polyethylenes synthesised using sMAO- $\text{Me}_2\text{SB}(\text{Cp},\text{I}^*)\text{Zr}(\text{CH}_2\text{Ph})_2$  (**4<sub>sMAO</sub>**) on the larger scale. Polymerisation conditions:  $[\text{Al}]_0:[\text{Zr}]_0 = 200:1$ , 2 bar ethylene, 250 mL hexane, 10 mg pre-catalyst, 750 mg TIBA, 30 minutes.

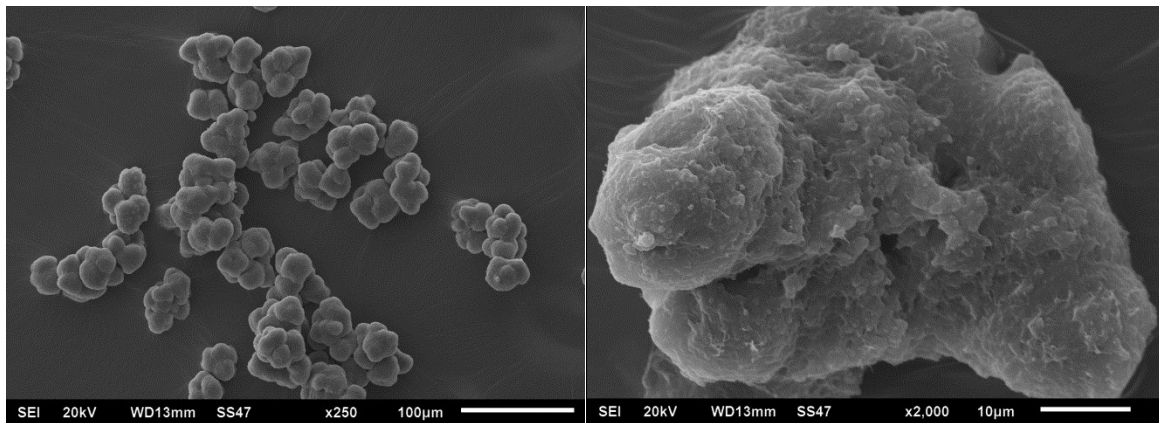


**Fig. S51.** SEM images of the polyethylenes synthesised using sMAO- $\text{Me}_2\text{SB}(\text{Cp}^{\text{Me}},\text{I}^*)\text{Zr}(\text{CH}_2\text{Ph})_2$  (**5<sub>sMAO</sub>**) on the larger scale. Polymerisation conditions:  $[\text{Al}]_0:[\text{Zr}]_0 = 200:1$ , 2 bar ethylene, 250 mL hexane, 10 mg pre-catalyst, 750 mg TIBA, 30 minutes.

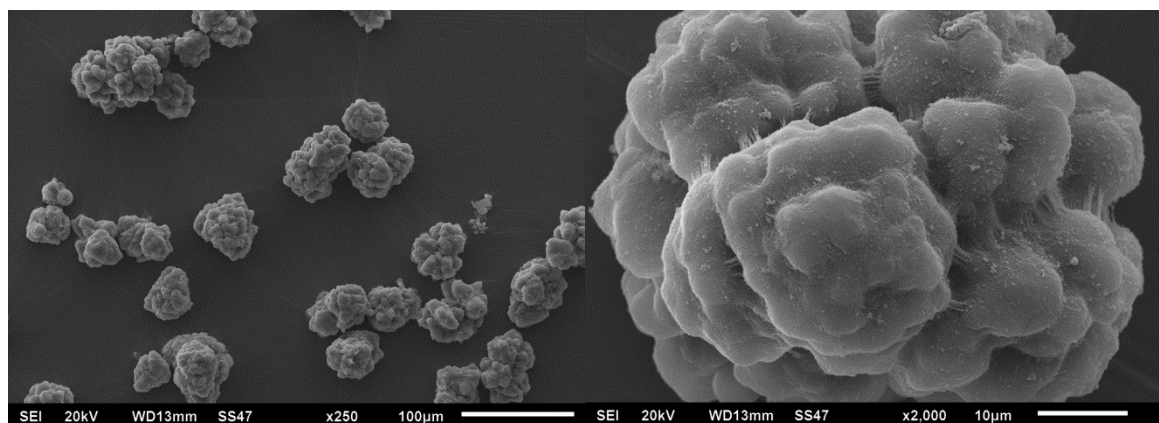


**Fig. S52.** SEM images of the polyethylenes synthesised using sMAO- $\text{Me}_2\text{SB}(\text{Cp},\text{I}^*)\text{ZrMe}_2$  (**6<sub>sMAO</sub>**) on the larger scale. Polymerisation conditions:  $[\text{Al}]_0:[\text{Zr}]_0 = 200:1$ , 2 bar ethylene, 250 mL hexane, 10 mg pre-catalyst, 750 mg TIBA, 30 minutes.

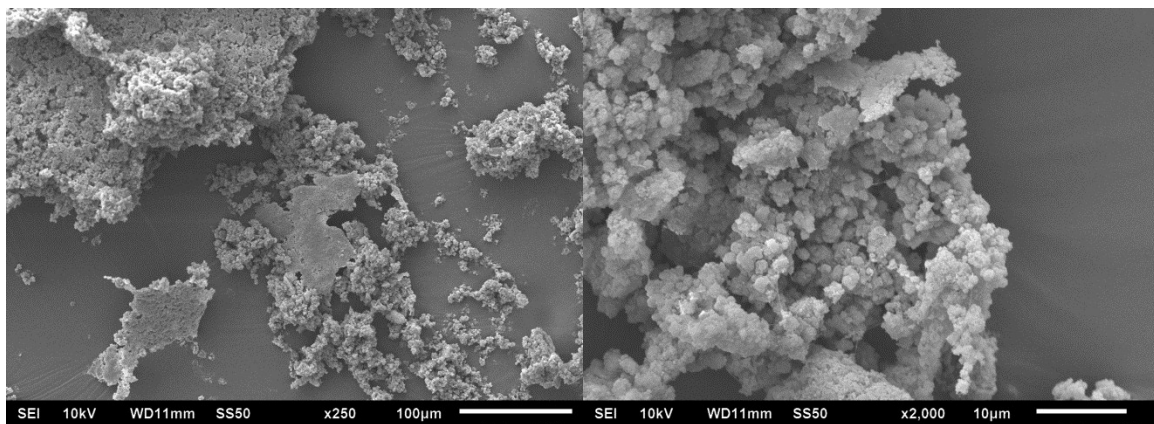


**Fig. S53.** SEM images of the polyethylenes synthesised using LDHMAO- $\text{Me}_2\text{SB}(\text{Cp},\text{I}^*)\text{ZrCl}_2$  (**A<sub>LDHMAO</sub>**). Polymerisation conditions:  $[\text{Al}]_0:[\text{Zr}]_0 = 200:1$ , 2 bar ethylene, 50 mL hexane, 10 mg pre-catalyst, 150 mg TIBA, 30 minutes.

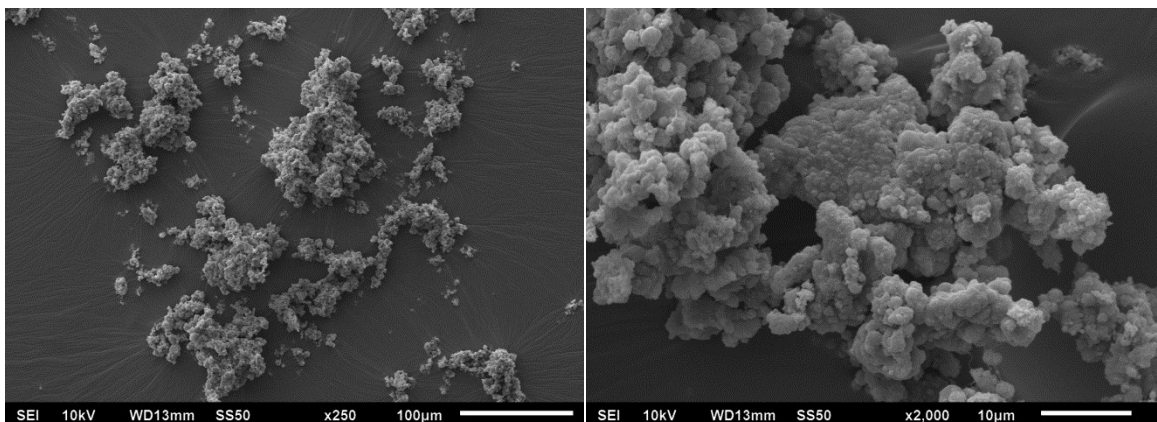


**Fig. S54.** SEM images of the polyethylenes synthesised using LDHMAO- $\text{Me}_2\text{SB}(\text{Cp}^{\text{Me}},\text{I}^*)\text{ZrCl}_2$  (**B<sub>LDHMAO</sub>**). Polymerisation conditions:  $[\text{Al}]_0:[\text{Zr}]_0 = 200:1$ , 2 bar ethylene, 50 mL hexane, 10 mg pre-catalyst, 150 mg TIBA, 30 minutes.

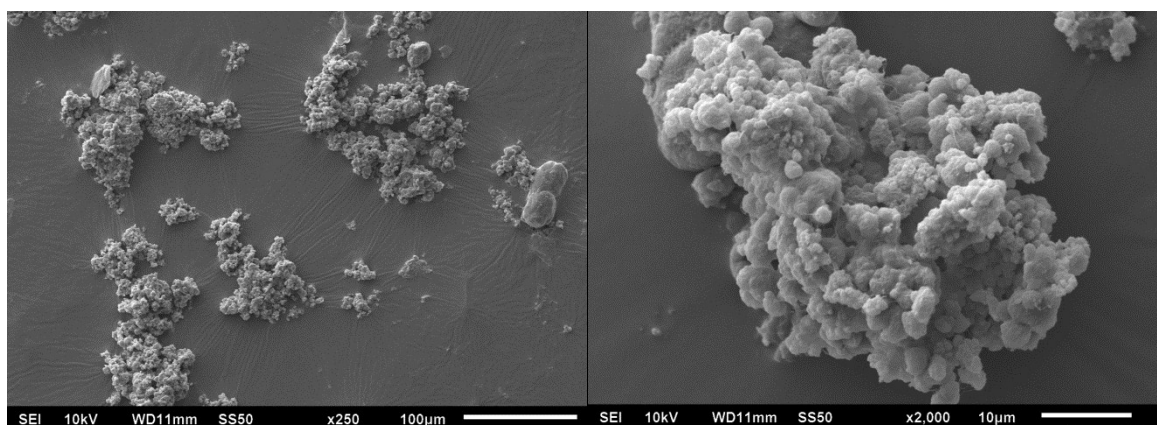


**Fig. S55.** SEM images of the polyethylenes synthesised using LDHMAO- $\text{Me}_2\text{SB}(\text{Cp},\text{I}^*)\text{Zr}(\text{CH}_2\text{Ph})_2$  (**4<sub>LDHMAO</sub>**). Polymerisation conditions:  $[\text{Al}]_0:[\text{Zr}]_0 = 200:1$ , 2 bar ethylene, 50 mL hexane, 10 mg pre-catalyst, 150 mg TIBA, 30 minutes.

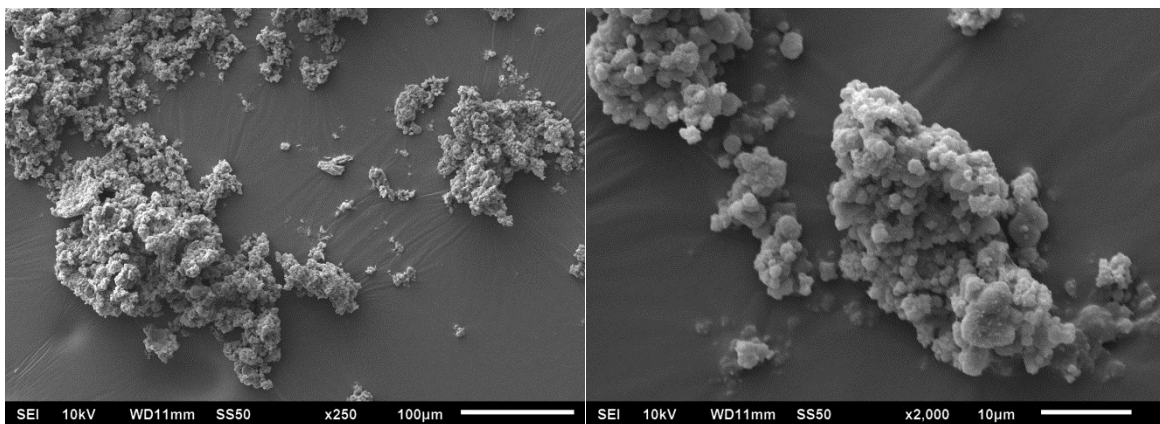


**Fig. S56.** SEM images of the polyethylenes synthesised using LDHMAO- $\text{Me}_2\text{SB}(\text{Cp},\text{I}^*)\text{ZrMe}_2$  (**6LDHMAO**). Polymerisation conditions:  $[\text{Al}]_0:[\text{Zr}]_0 = 200:1$ , 2 bar ethylene, 50 mL hexane, 10 mg pre-catalyst, 150 mg TIBA, 30 minutes.

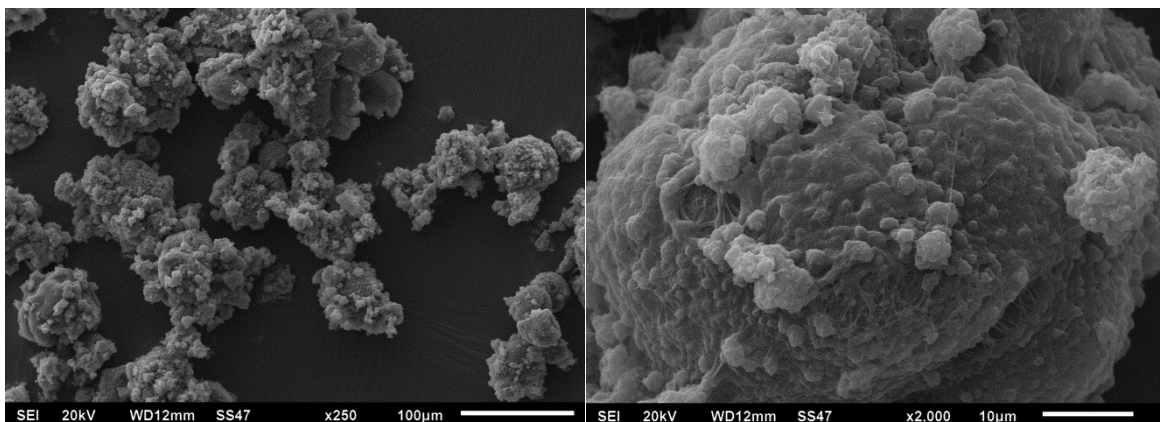


**Fig. S57.** SEM images of the polyethylenes synthesised using SSMAO- $\text{Me}_2\text{SB}(\text{Cp},\text{I}^*)\text{ZrCl}_2$  (**ASSMAO**). Polymerisation conditions:  $[\text{Al}]_0:[\text{Zr}]_0 = 200:1$ , 2 bar ethylene, 50 mL hexane, 10 mg pre-catalyst, 150 mg TIBA, 30 minutes.

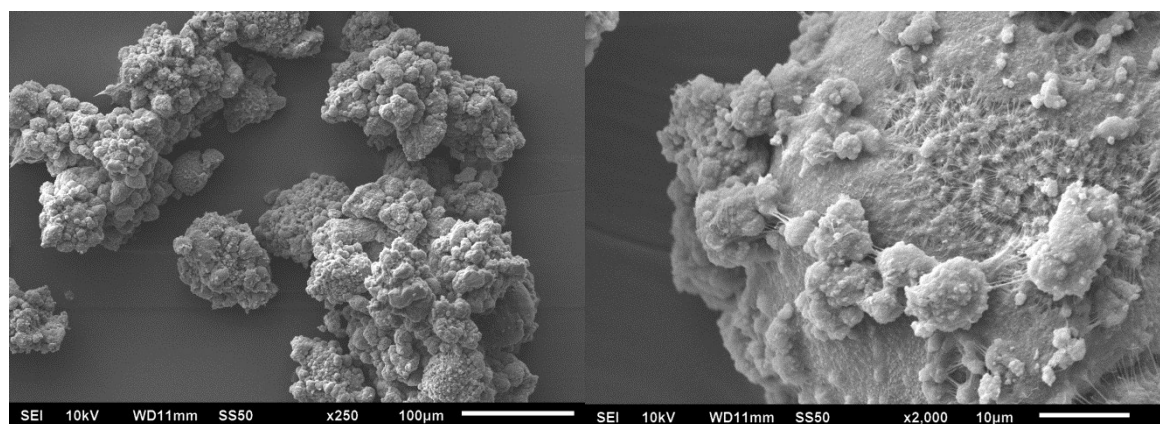


**Fig. S58.** SEM images of the polyethylenes synthesised using SSMAO- $\text{Me}_2\text{SB}(\text{Cp}^{\text{Me}},\text{I}^*)\text{ZrCl}_2$  (**BSSMAO**). Polymerisation conditions:  $[\text{Al}]_0:[\text{Zr}]_0 = 200:1$ , 2 bar ethylene, 50 mL hexane, 10 mg pre-catalyst, 150 mg TIBA, 30 minutes.

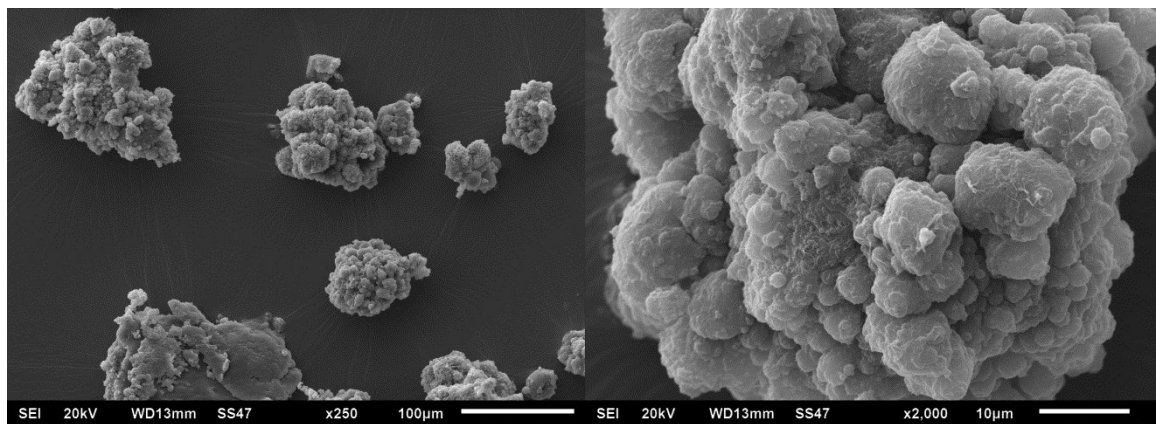


**Fig. S59.** SEM images of the polyethylenes synthesised using SSMAO- $\text{Me}_2\text{SB}(\text{Cp},\text{I}^*)\text{Zr}(\text{CH}_2\text{Ph})_2$  (**4<sub>SSMAO</sub>**). Polymerisation conditions:  $[\text{Al}]_0:[\text{Zr}]_0 = 200:1$ , 2 bar ethylene, 50 mL hexane, 10 mg pre-catalyst, 150 mg TIBA, 30 minutes.

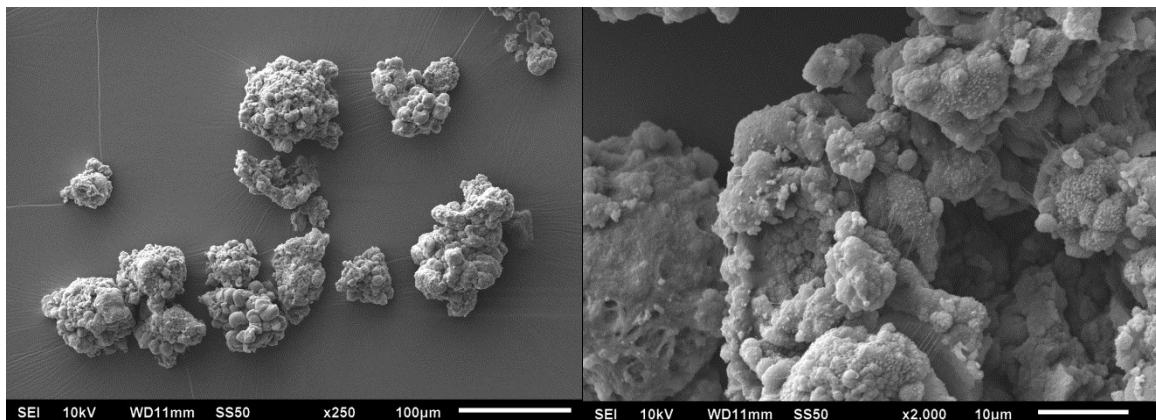


**Fig. S60.** SEM images of the polyethylenes synthesised using SSMAO- $\text{Me}_2\text{SB}(\text{Cp},\text{I}^*)\text{ZrMe}_2$  (**6<sub>SSMAO</sub>**). Polymerisation conditions:  $[\text{Al}]_0:[\text{Zr}]_0 = 200:1$ , 2 bar ethylene, 50 mL hexane, 10 mg pre-catalyst, 150 mg TIBA, 30 minutes.

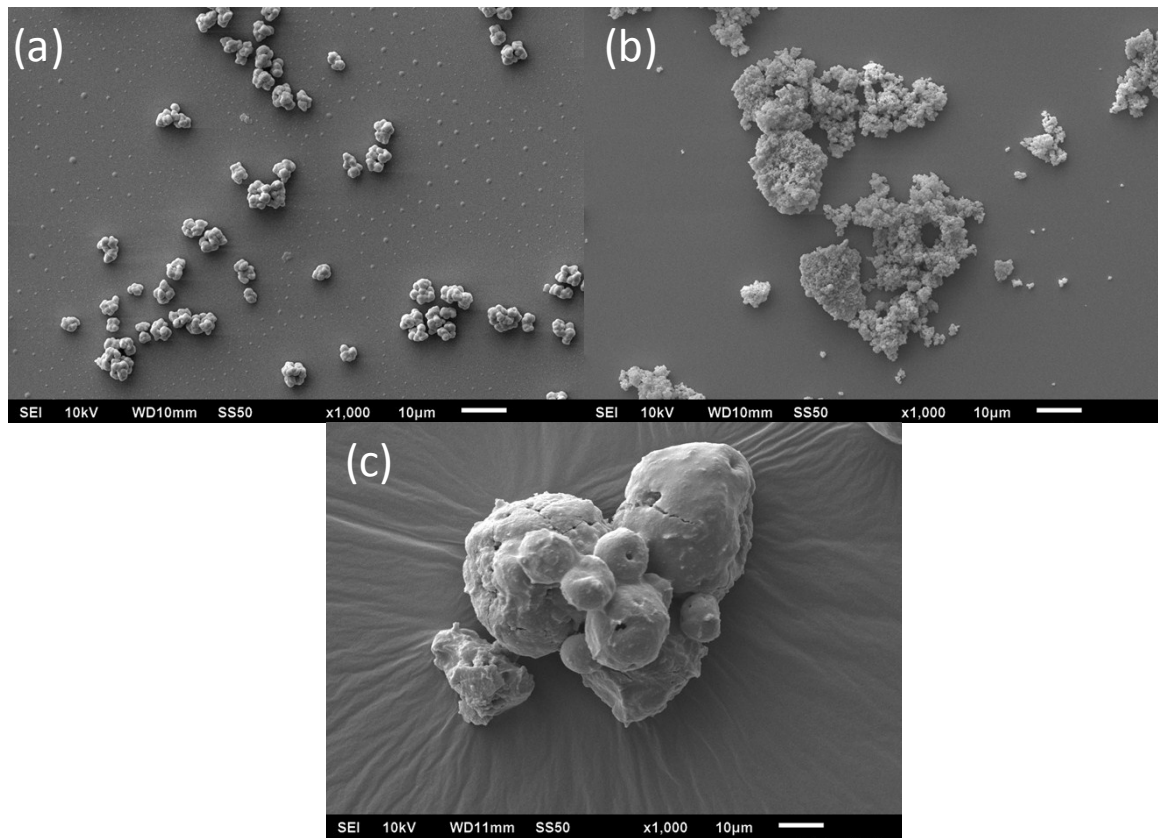


**Fig. S61.** SEM images (a) sMAO, (b) LDHMAO and (c) SSMAO.

## **5. References**

1. J. Cosier and A. M. Glazer, *Journal of Applied Crystallography*, 1986, **19**, 105-107.
2. CrysAlisPRO, Oxford Diffraction /Agilent Technologies UK Ltd, Yarnton, England.
3. A. Altomare, G. Cascarano, C. Giacovazzo and A. Guagliardi, *Journal of Applied Crystallography*, 1993, **26**, 343-350.
4. L. Palatinus and G. Chapuis, *Journal of Applied Crystallography*, 2007, **40**, 786-790.
5. L. Farrugia, *Journal of Applied Crystallography*, 1999, **32**, 837-838.
6. L. J. Farrugia, *Journal of Applied Crystallography*, 2012, **45**, 849-854.
7. A. L. Spek, *Journal of Applied Crystallography*, 2003, **36**, 7-13.
8. A. L. Spek, *PLATON, a Multipurp. Crystallogr. tool, Utrecht, Netherlands*, 1998.